LBNL-41429
Preprint

ERNEST ORLANDO LAWRENCE
BERKELEY NATIONAL LABORATORY

Neutron Yields from 435 MeV/Nucleon Nb Stopping in Nb and 272 MeV/Nucleon Nb Stopping in Nb and Al

L. Heilbronn, R. Madey, M. Elaasar, M. Htun, K. Frankel, W.G. Gong, B.D. Anderson, A.R. Baldwin, J. Jiang, D. Keane, M.A. McMahan, W.H. Rathbun, A. Scott, Y. Shao, J.W. Watson, G.D. Westfall, S. Yennello, and W.M. Zhang

Life Sciences Division

February 1998

Submitted to
Physical Review C

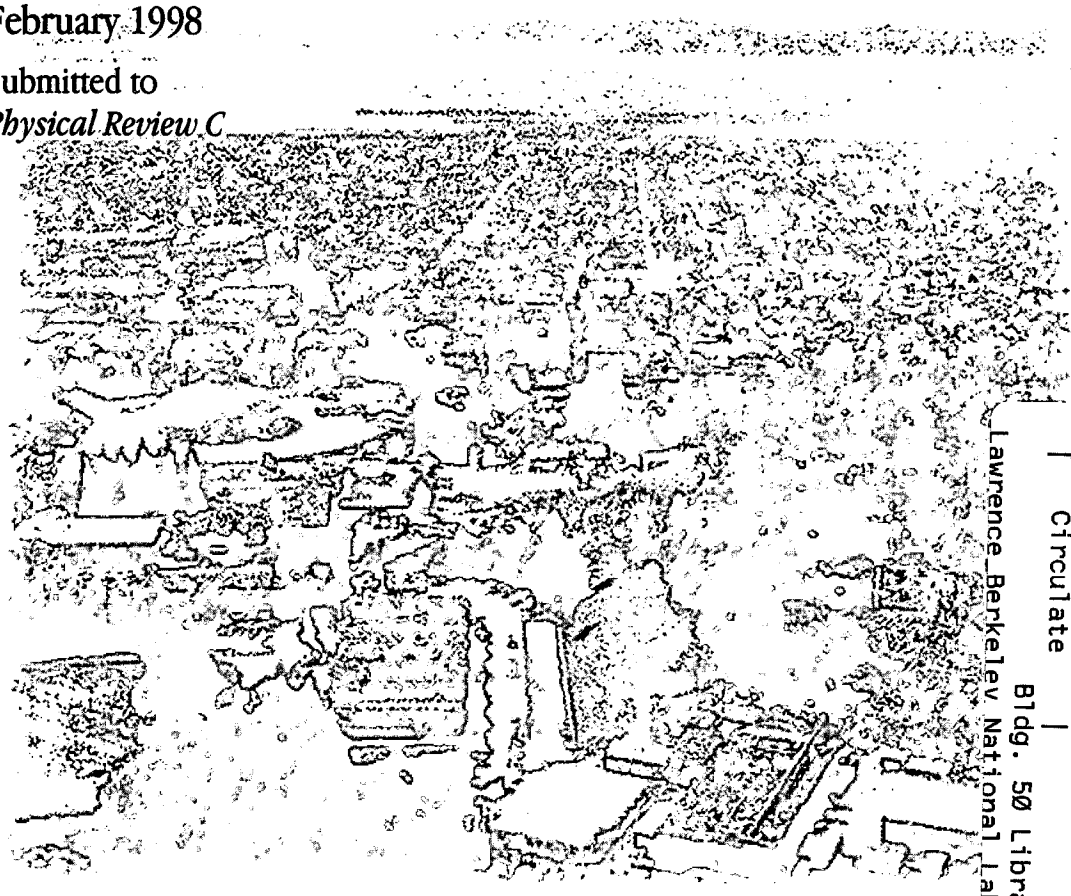

DISCLAIMER

LBNL-41429

Neutron Yields from 435 MeV/Nucleon Nb Stopping in Nb and 272 MeV/Nucleon Nb Stopping in Nb and Al

L. Heilbronn,[1] R. Madey,[2] M. Elaasar,[2,a] M. Htun,[2,b] K. Frankel,[1] W.G. Gong,[3] B.D. Anderson,[2] A.R. Baldwin,[2] J. Jiang,[2,c] D. Keane,[2] M.A. McMahan,[1] W.H. Rathbun,[1] A. Scott,[2,d] Y. Shao,[2,e] J.W. Watson,[2] G.D. Westfall,[4] S. Yennello,[4,f] and W.M. Zhang[2]

[1]Life Sciences Division
Ernest Orlando Lawrence Berkeley National Laboratory
University of California
Berkeley, California 94720

[2]Kent State University
Kent, Ohio 44242

[3]MPI, Foehringer Ring 6
D-80805 Munich, Germany

[4]Michigan State University
East Lansing, Michigan 48824

February 1998

[a]Southern University, New Orleans, LA
[b]CyberAccess, Inc., Valley View, OH 44125
[c]Picker International, Solon, OH
[d]Department of Physics, University of Wisconsin-Stout, Menomonie, WI
[e]Crump Institute for Biological Imaging, UCLA, Los Angeles, CA 90095-6948
[f]Department of Chemistry, Texas A&M University, College Station, TX 77843

This work was supported in part by the National Science Foundation under Grant Nos. PHY-96-05207, PHY-91-07064, PHY-88-02392, and PHY-86-11210, the U.S. Department of Energy under Contract Nos. DE-FG89ER40531 and DE-AC03-76SF00098, and the National Aeronautics and Space Administration under NASA Grant L14230C.

ABSTRACT

Neutron fluences were measured from 435 MeV/nucleon Nb ions stopping in a Nb target and 272 MeV/nucleon Nb ions stopping in targets of Nb and Al for neutrons above 20 MeV and at laboratory angles between 3° and 80°. The resultant spectra were integrated over angle to produce neutron energy distributions; and over energy to produce neutron angular distributions. The total neutron yields for each system were obtained by integrating over the angular distributions. The angular distributions from all three systems are peaked forward and the energy distributions from all three systems show an appreciable yield of neutrons with velocities greater than the beam velocity. Comparisons of the total neutron yields from all three systems suggest that the yield scales with the fraction of Nb ions interacting in the target; however, data for neutrons below 20 MeV are needed to relate the number of interaction lengths and the total neutron yield. The data are compared with BUU model calculations.

I. INTRODUCTION

Neutron spectra produced by 435 MeV/nucleon Nb ions stopping in a Nb target and by 272 MeV/nucleon Nb ions stopping in Al and Nb targets were measured at the Lawrence Berkeley Laboratory's Bevalac facility. The spectra reported here are for neutrons with energies from 20 MeV up to twice the beam energy (in MeV/nucleon), and for laboratory angles between 3 and 80 degrees. These measurements were motivated by the desire to provide some insight into the nature of the neutron spectra produced by interactions of high-energy heavy-ions ($Z \geq 3$, referred to as HZE) present in Galactic Cosmic Rays (GCR) with shielding materials used to protect humans engaged in long-term missions outside the geomagnetosphere. Data are useful also to the heavy-ion radiotherapy community, where the calculation of the dose delivered inside the patient must take into account the flux of neutrons produced by the interactions inside the patient.

Because there are essentially no free neutrons in the primary GCR, the only significant source of neutrons is from interactions of the primary GCR with shielding materials. The yield of neutrons behind thick shielding is especially important because (1) interactions of the primary GCR in those shields produce neutrons that make up a sizable fraction of the particles behind the shielding [1], and (2) neutrons have relatively high weighting factors in terms of their potential to inflict biological damage [2]. One calculation predicts that close to 50% of the dose-equivalent behind shielding comprised of 50 g/cm^2 of Martian regolith comes from neutrons [1]. Although HZE particles make up just 1% of the GCR (with 87% protons, and 12% alphas [3]), similar calculations have shown that approximately 16% of the neutron flux behind 50 g/cm^2 of water comes from the fragmentation of HZE; another 15% comes from interactions with GCR alpha particles, with the remainder from proton-induced interactions [4].

The transport models [4], [5] used in the calculations mentioned above and in other similar calculations (such as Monte-Carlo codes used in heavy-ion radiotherapy problems) need cross section data for input into the codes and thick-target data for verification of the models' output.

Because the GCR encompass a wide range of particles (from protons up to iron, with some flux of ions heavier than iron) and a wide range of kinetic energies (with most of the GCR flux contained between 100 and 2000 MeV/nucleon), the set of data needed by those models will need to cover a significant portion of the range of ions and energies present in the GCR. Also, the data set will need to include targets that cover the broad range of possible shielding materials and tissue components. There are data sets of neutron production cross-sections [6 - 11] from HZE interactions, and there are data on the production of neutrons from 177.5 and 160 MeV/nucleon alphas stopping in various targets [12]; however, there are few, if any, data sets of neutrons produced by HZE (with $Z > 2$) interactions in stopping targets.

The data presented here are intended to describe the general nature of neutrons produced by the interactions of the heavier constituents of the GCR in a stopping target. This description includes such properties as the angular and energy distributions, the total yields, and the dependence of the yield on target mass and projectile energy. Details of the experiment follow in section II, with the data analysis and discussion in sections III and IV. Comparisons of the data with a model that uses BUU-generated cross sections are in section V.

II. EXPERIMENTAL DETAILS

The data presented here come from a neutron time-of-flight experiment that was done at the Bevalac Facility at Lawrence Berkeley Laboratory. This experiment was an adjunct to experiment E848H [13]. The choice of beams was dictated by the physics goals of the primary experiment; hence, the choice of Nb for both the 435 and 272 MeV/nucleon beams. Although Nb is not a significant component of the GCR, the reaction mechanisms producing neutrons in the systems used here are typical of heavy-ion reactions in this energy domain, and as such, the data reported here can be used to test models that calculate neutron production from HZE GCR-like ions. Beam was delivered in one-second long spills every six seconds, with approximately 3×10^5 particles per spill on target. Two beam-defining scintillators were placed upstream from the target for the purpose of identifying beam particles focused on target with a minimum divergence. A valid beam particle was defined by the coincidence between the two scintillators.

The data came from 14 neutron detectors placed between 3° and 80° in the lab. Each neutron detector was a 10.16-cm-thick rectangular slab of NE-102. All 14 detectors were 101.6 centimeters in height. The widths of the detectors varied from detector to detector. Table I lists the angle, dimensions, flight path, and solid angle of each detector. Each detector was placed such that the center of the detector was at the same height as the target. Pulse-height calibrations were carried out with a ^{228}Th source, a precision amplifier with a gain of 10, and attenuators with attenuation factors of 2, 5, and 10. The pulse-height response was linear and stable over the entire time of the experiment. Directly in front of each neutron detector was a 6.4-mm-thick NE-102 scintillator with a height and width slightly larger than the neutron detector. This scintillator was used to reject any charged particles from the target that were incident on the neutron detector.

A 1-cm-thick (8.57 g/cm^2) Nb target was used for the 435 MeV/nucleon run, and a 0.51-cm-thick (4.37 g/cm^2) Nb target and a 1.27-cm-thick (3.43 g/cm^2) Al target were used for the 272

TABLE I

lab angle (deg)	height (cm)	width (cm)	flight path (cm)	solid angle (msr)
3.0	100.0	2.5	840.	0.36
6.0	100.0	2.5	840.	0.36
9.0	100.0	12.7	840.	1.80
12.0	100.0	12.7	840.	1.80
16.0	100.0	25.4	840.	3.60
20.0	100.0	25.4	840.	3.60
24.0	100.0	25.4	840.	3.60
28.0	100.0	25.4	840.	3.60
32.0	100.0	25.4	840.	3.60
36.0	100.0	25.4	840.	3.60
40.0	100.0	50.8	840.	7.20
48.0	100.0	50.8	800.	7.94
56.0	100.0	50.8	750.	9.03
64.0	100.0	50.8	700.	10.37
72.0	100.0	50.8	620.	13.22
80.0	100.0	50.8	600.	14.11

Table I. Information on the position of the neutron detectors used in this experiment. All detectors are 10.16-cm thick. The flight paths are measured relative to the center of the detector.

MeV/nucleon runs. All the targets were thick enough to stop the beam. The targets were housed in a scattering chamber that had a thin mylar window positioned between the target and neutron detectors.

III. DATA ANALYSIS

A. Neutron Energy Determination and Flux Corrections

Neutron energies were determined by measuring the time of flight between a signal from the beam particle telescope and a mean-timed [14] signal from the neutron detector. An absolute time scale in each one of the resulting 14 TDC spectra was determined by measuring the position of the prompt gamma-ray peak. The timing resolution for the 435 MeV/nucleon run, as measured by the width (FWHM) of the prompt gamma-ray peak, varied from 0.8 to 1.4 ns depending on the detector used; the timing resolution increased for the 272 MeV/nucleon runs to values between 1.4 and 1.7 ns. The raw TDC data for each detector and each run was rebinned such that the minimum bin width was at least the size of the appropriate timing resolution. Energy spectra were then produced from the rebinned TDC spectra.

The detection efficiency of each neutron detector was calculated using the code of Cecil et al. [15] Figure 1 shows the detection efficiency as a function of energy for the four sizes of detectors used in this experiment, with a pulse-height threshold of 10 MeV in equivalent electron energy, which is equivalent to about 18 MeV in neutron energy.

Corrections to the data were needed also to adjust for the loss of neutron flux from the presence of scattering materials between the target and the neutron detector. The amount of neutron flux lost by scattering was calculated with a code containing the appropriate neutron scattering cross sections and scattering materials. There was a wall of plastic scintillators mounted on a wooden frame placed between the target and neutron detectors at forward angles, and just in front of the scintillator wall was a thin sheet of steel used for delta-ray suppression. Although the data from the scintillator wall are not presented in this analysis, those materials were present at all times and the loss of neutron flux through them must be taken into account. The air between the target and neutron detectors also contributed to the loss of neutron flux, and was included in the flux-transmission calculations. Shown in Fig. 2 as a function of neutron energy is the fraction of neutron flux transmitted from the target to the detectors between 3° and 20° (air + wood + plastic scintillator wall + steel + veto scintillator, shown with the solid line), 24° and 36° (air + wood + wall scintillator + veto scintillator, shown with the dashed line) and 48° and 80° (air + veto scintillator, shown with the dotted line).

B. Background Estimation

Because of the limited amount of beam time available for the measurements, background neutrons were not measured with shadow shields in place; instead, the background was estimated from particular regions in the TDC spectra where none of the events were generated by neutrons

coming directly from the target. Figure 3 shows a TDC spectrum for the detector at 3° gated on pulse heights above 8 MeV of equivalent electron energy. The peak labeled A is the prompt gamma-ray peak. Time increases from left to right; thus, all neutrons coming directly from the target will be to the right of the gamma-ray peak.

The counts to the left of the gamma ray peak are from uncorrelated, out-of-time events. One source of these out-of-time events is cosmic-rays that strike the neutron detector but do not pass through the accompanying veto detector. The distribution of counts in this region (referred to hereon as "Region I") was flat in all cases. It is assumed that these out-of-time events will extend over the entire range of the TDC spectrum with a constant magnitude.

The channel marked B (channel number 1474) in Fig. 3 indicates the location in the TDC spectrum where the pulse height threshold takes effect. Any counts to the right of channel B cannot come directly from the target because their time of flight has a corresponding energy that is below threshold. Instead, those events are out-of-time events which are also seen exclusively in Region I, and target-induced background from room-scattered neutrons and gammas which are not present in Region I; accordingly the average number of counts to the right of channel B (referred to as "Region II") should exceed the average number of counts in Region I, which is the case for all detectors and for all pulse-height thresholds used. The distribution of counts in Region II was flat for all detectors and thresholds used in the analysis.

There is no direct way to determine the shape and magnitude of the background spectrum between points A and B in Fig. 3; consequently, it is necessary to assume a background shape in that area and use the information available from regions I and II to determine the magnitude of that background. Two types of background shapes were assumed in this analysis, and the final background values were found by averaging over the two types.

One of the background shapes is similar to the one used in Ref. [12] and is shown with + symbols in Fig. 3; this type I background is assumed to be flat (with a magnitude equal to the average number of counts in Region II) from the threshold channel to the channel that corresponds to the flight time for a floor-scattered neutron coming from the target, with an energy equal to that of the high-energy peak in the TDC spectrum. The background is then assumed to decrease linearly from the floor-scattered channel down to the gamma peak postion. The magnitude of the background at the gamma peak postion is equal to the average number of counts in Region I.

The second type of background (for neutrons coming from the target that scatter from the floor, ceiling, and walls into a particular detector) assumes a shape to be the same as the measured spectrum; also, the background spectrum would be shifted along the x-axis because the flight paths for background neutrons are longer than for neutrons coming directly from the target. Thus, for a particular neutron detector, the second type of background is calculated by (1) taking the measured TDC spectrum of that detector and multiplying it by a fixed percentage, and then (2) shifting the TDC channel number to account for the longer flight times of room-scattered neutrons. The amount of the shift was calculated for the flight path of a neutron scattered from a point on the floor halfway between the target and the neutron detector. The fixed percentage was determined by setting the average number of counts in the assumed background TDC spectrum in Region II equal to the average number of counts in Region II of the measured TDC spectrum,

where all the events in Region II are background events. The fixed percentages varied from 5% to 15%, depending on the detector and reaction system used. The open symbols in Fig. 3 show the type 2 background.

As can be seen in Fig. 3, the type 1 and type 2 backgrounds serve as the lower and upper bounds, respectively, in the background estimation. The dashed line in Fig. 3 shows the averaged-background contribution to that spectrum. The background contribution was greatest at the lowest energies (20 to 30 MeV), where the background contributions varied between 7 percent for the detector at 72° and 32 percent for the detector at 3°. The disparity between the two types of backgrounds is greatest for the highest energy neutrons, where the magnitudes of the backgrounds varied by as much as a factor of 1000 at the forward angles; although this disparity is large, the uncertainty in the background at these points contributed only 6 to 8 percent in the overall uncertainty in the neutron spectra there.

IV. EXPERIMENTAL RESULTS

A. Double Differential Spectra

Shown in Figs. 4, 5, and 6 are neutron energy spectra for the 435 MeV/nucleon Nb + Nb system, the 272 MeV/nucleon Nb + Nb system, and the 272 MeV/nucleon Nb + Al system, respectively. The uncertainties shown in the figures include the statistical uncertainties and the uncertainties from background subtraction. Error bars are emitted when the uncertainty is smaller than the size of the plotting symbol. Spectra are shown for the detectors at 3°, 9°, 16°, 28°, 48°, and 80°. The yields in these stopping-target spectra are expressed in units of the number of neutrons per MeV per unit solid angle per incident Nb ion. In all cases, the low-energy threshold was 20 MeV. The solid lines shown in Figs. 4 - 6 represent Boltzmann-Uehling-Uhlenbeck calculations. The details of those calculations are described in section V. The dashed lines are a parameterization of the large-angle data, as explained later in this section.

Table A-I, located at the end of this report, contains the spectra from all 14 angles for the 435 MeV/nucleon Nb + Nb system. Each angle is indicated in the table. Tables A-II and A-III, also at the end of this report, contain the spectra from all 14 angles for the 272 MeV/nucleon Nb + Nb and Nb + Al systems, respectively.

Projectile fragmentation is the dominant mechanism for the production of neutrons at forward angles [16, 17], as can be seen in Figs. 4-6 by the relative abundance of high-energy neutrons at those angles. One striking difference between the forward-angle spectra from stopping and thin targets is that the stopping-target spectra show a broad peak of projectile-like neutrons extending from about one-third of the beam energy per nucleon up to an energy approximately ten to twenty percent above the incident beam energy per nucleon, whereas thin-target forward-angle spectra show a much narrower peak centered near the incident beam energy per nucleon (see, for example, Ref. [6, 18]). The difference arises from the fact that the interactions in the stopping target occur over a range of projectile energies extending from the incident beam energy per nucleon down to

TABLE II

	Nb + Nb 435 MeV/nucleon	Nb + Nb 272 MeV/nucleon	Nb + Al 272 MeV/nucleon
28°	121	81	77
48°	88	61	60
80°	62	42	40

Table II. Values of the slope parameter $< E_o >$ used in Equation 1 to fit the spectra for the systems and angles indicated. The fits are shown as dashed lines in Figs. 4 - 6. $< E_o >$ is in units of MeV.

energies reached just before stopping in the target, while the thin target reactions occur essentially over one projectile energy. Based on the assumption that the deviation of the spectral shapes from a straight exponential fall off is due primarily to projectile-like neutrons, contributions to the spectra from projectile-like neutrons can be seen qualitatively out to 9° in Fig. 4 and out to 16° in the 272 MeV/nucleon systems.

At larger angles ($\theta \geq 28°$) the spectra in all three cases are dominated by neutrons coming from the decay of the overlap region, or "mixing" region, of projectile and target nucleons. The spectra there show the same characteristics of particle production from the overlap region as seen in thin-target spectra [6, 18], such as the exponential fall-off with energy and the increase in the steepness of the slopes as the laboratory angle increases. As with thin-target spectra, the large angle stopping-target spectra can be represented with a simple exponential of the form

$$y = N * \exp(-E_n / < E_o >), \tag{1}$$

where y is the number of neutrons per MeV per unit solid angle per incident ion at a particular angle and neutron energy E_n, N is a normalization constant, and $< E_o >$ is the slope parameter. Because interactions in the stopping target occur at all projectile energies from the incident energy on down, $< E_o >$ is not a parameter that describes the interactions at one particular projectile energy (as is the case when thin-target data are fitted with the same form of exponential [19].), but is rather a weighted average of the slope parameters over the entire range of interactions. Table II shows the values of $< E_o >$ for the systems and angles indicated, and the dashed lines in Figs. 4 - 6 show the fits to the data using Eqn. 1. Comparison of the large-angle spectra from 435 MeV/nucleon system and the 272 MeV/nucleon systems shows steeper slopes (smaller values of $< E_o >$) in the lower-energy systems, which is consistent with the systematics found in the analyses of thin-target heavy-ion data (see Fig. 2 of Ref. [19], and references contained therein). A similar comparison between the two 272 MeV/nucleon systems shows that the mass of the target makes no significant difference on the spectral slopes at large angles.

B. Energy Distributions

Because neutrons coming from the decay of a target-like source dominate the spectra at low energies and at large angles, much of the contribution from target-like neutrons is missing in the three spectra; the reason is the relatively high (20 MeV) neutron-energy threshold of the spectra and the relatively forward placement ($\theta \leq 80°$) of the neutron detectors. The significance of the missing target-like neutrons can be seen in the left-hand plots in Fig. 7 which show the energy-dependent neutron yields after integrating the experimental neutron spectra from 0° to 90° for all three systems. The data are expressed in units of the number of neutrons per MeV per incident Nb ion. For all three systems, the spectra fall off with increasing neutron energy. Although the yield below threshold cannot be determined, the trend of the data shows that there is potentially a large yield of mostly target-like neutrons below threshold. This point is important to consider when total neutron yields are extracted (see subsection D below) from these data.

C. Angular Distributions

The right-hand plots in Fig. 7 show the angular distributions for the indicated systems for all 14 angles and for neutron energies above 20 MeV. The data are expressed in units of the number of neutrons per unit solid angle per incident Nb ion. The uncertainties shown include an assumed 10 percent scale uncertainty in the efficiency calculation and an assumed five percent scale uncertainty in the attenuation calculation. Readily evident in all three spectra is that angular distributions are enhanced strongly in the forward direction. The solid lines show a fit to the data based on a superposition of two exponentials:

$$y = a_1 * \exp(-a_2 * \theta) + a_3 * \exp(-a_4 * \theta), \tag{2}$$

where a_1, a_2, a_3, and a_4 are fit parameters and y is the number of neutrons per msr. Qualitatively, the two exponentials represent the separate contributions to the angular distributions from projectile-like neutrons and neutrons from the decay of overlap region.

The contributions to the fit from each exponential can be seen with the dotted ($a_3 * \exp(-a_4 * \theta)$) and dashed ($a_1 * \exp(-a_2 * \theta)$) lines. Table III shows the fit parameters for all three systems where the angle θ is expressed in degrees. The contribution from forward-focussed neutrons ($a_3 * \exp(-a_4 * \theta)$) shows a rapid falloff with laboratory angle, although the falloff is not as rapid in the 272 MeV/nucleon systems as it is in the 435 MeV/nucleon system. It is assumed that the forward-focussed neutrons come primarily from the breakup of the projectile remnant, and the other neutrons (described with the other term in Eqn. 2, $a_1 * \exp(-a_2 * \theta)$), come primarily from the decay of the overlap region. The point where there are equal contributions from projectile-like and overlap neutrons is around 9° for the 435 MeV/nucleon system, and is around 12° for the 272 MeV/nucleon systems. The greater contribution from projectile-like neutrons at larger angles in the 272 MeV/nucleon systems is consistent with the decrease of the beam momentum per nucleon in those systems as compared to the 435 MeV/nucleon system. There is approximately a 25% change in momentum per nucleon going from the 435 MeV/nucleon system to the 272 MeV/nucleon system, and this leads to the observed 25% change in the point where there are equal contributions from the two sources (assuming there is no significant change in the transverse momentum between the two systems). Other than the overall normalization, there is no significant difference in the angular distributions between the two 272 MeV/nucleon systems.

TABLE III

	Nb + Nb 435 MeV/nucleon	Nb + Nb 272 MeV/nucleon	Nb + Al 272 MeV/nucleon
a_1 (neutrons/MeV incident-ion)	0.00541	0.00179	0.00244
a_2 (1/deg)	0.0522	0.0517	0.0593
a_3 (neutrons/MeV incident-ion)	0.0899	0.0237	0.0366
a_4 (1/deg)	0.413	0.295	0.0286

Table III. Fit parameters from Equation 2 for all three systems. The angle θ in Equation 2 is in units of degrees.

TABLE IV

System	0° - 90°	0° - 45°	0° - 10°	% interacted
Nb + Nb 435 MeV/nucleon	4.5 ± 0.5	3.5 ± 0.4	1.3 ± 0.2	23
Nb + Nb 272 MeV/nucleon	1.7 ± 0.2	1.4 ± 0.2	0.54 ± 0.06	11.6
Nb + Al 272 MeV/nucleon	2.1 ± 0.3	1.9 ± 0.2	0.8 ± 0.1	19

Table IV. Total neutron yields (in neutrons per incident ion) for the given systems and the given angular ranges. The numbers in the last column give the expected percentage of incoming ions that undergo a nuclear interaction, as determined from an energy-dependent total cross section calculation.

D. Total Yields

Table IV shows the total yields of neutrons above 20 MeV for all three systems expressed in units of the number of neutrons per incident Nb ion. The total yields are obtained by integrating the angular distributions from 0° to 90°; thus, the numbers in the second column of Table IV represent the number of neutrons above 20 MeV emitted in the foward 2π steradians. The numbers in the third and fourth columns in Table IV are the number of neutrons above 20 MeV emitted in the first 45 degrees and the first ten degrees, respectively. The last column in Table IV indicates the percentage of incoming Nb ions expected to undergo a nuclear interaction before stopping, as calculated by stepping the incident ion through successive layers of target and using the appropriate energy-dependent geometric cross section at each layer. The uncertainties include the statistical and scale uncertainties discussed above.

The ratio of the total yield of the 272 MeV/nucleon Nb + Nb system to the yield of the 435

MeV/nucleon Nb + Nb system is 0.38 ± 0.06. Looking at the values in the percent-interacted column, one might expect the ratio to be 0.5, but the experimental value is two standard deviations lower than that; however, it may be unfair to compare the two systems because the same neutron energy threshold was applied to both data sets. The 272 MeV/nucleon system will have a larger percentage of its neutron flux in the undetected 0 - 20 MeV range than will the 435 MeV/nucleon system because the amount of energy available to produce neutrons in the 272 MeV/nucleon system is lower than the energy available in the 435 MeV/nucleon system, which in turn means that the spectra of neutrons produced in the 272 MeV/nucleon will be weighted towards lower kinetic energies than the spectra produced in the 435 MeV/nucleon system. If one could then add in the yield of neutrons below 20 MeV in both systems to the total yields, the ratio of the total yields would be expected to decrease, perhaps close to the expected value of 0.5. In any case, there clearly is a dependence of the total neutron yield on the energy of the incoming ion that seems to scale, to first order, with the number of interaction lengths required to stop the ion.

The ratio of the total yields of the 272 MeV/nucleon Nb + Nb system to the 272 MeV/nucleon Nb + Al system is 0.80 ± 0.14, whereas the ratio of the calculated percent-interacted is 0.61. If one weights the ratio of the expected percentage of interactions with the ratio of the total number of neutrons in each system (taken to be 104 neutrons for the Nb + Nb system and 66 neutrons for the Nb + Al system), the expected ratio of the two systems is 0.96, which is about 1.5σ above the experimental value; however, it may be misleading to include all of the target neutrons into the expected ratio because the relatively high neutron energy threshold excludes much of the contribution from target evaporation. If one instead just uses half of the target neutrons in the expected-ratio calculation (leaving 78 neutrons for the Nb + Nb system and 59 neutrons for the Nb + Al system), one gets an expected ratio of 0.81, which agrees with the experimental value. One other work has looked at the target dependence on stopping-target neutron yields for alpha bombardment of various targets at 177.5 MeV/nucleon, and they have found the that the integrated yields are independent of the target (0.5 neutrons per incident He ion) [12]. Within uncertainties, it can be said also that the total neutron yields are independent of the target in this work, although data below 20 MeV are needed here before a firm conclusion can be drawn in this regard.

As can be seen from the values in columns 3 and 4 of Table IV much of the total yield is forward focussed. Thirty percent of the flux in the Nb + Nb systems are contained within the first 10 degrees, while forty percent of the flux in the Nb + Al system is in the first 10 degrees. About 80 to 90 percent of the total flux between 0° and 90° is contained within the first 45 degrees for all three systems.

V. BUU MODEL COMPARISONS

Boltzmann-Uehling-Uhlenbeck (BUU) calculations have been compared with measured double-differential neutron cross sections; it is not possible, however, to take the output of such BUU calculations and directly compare them to stopping-target yields, such as the yields reported in

this work. Stopping-target yields involve interactions over a wide range of projectile energies and may include a significant contribution from the interactions of secondaries within the target. Because these effects are not contained in any one BUU calculation, we employed a simple technique that builds up stopping-target yields from cross sections produced by BUU model calculations.

The first step was to transport the incident Nb ion through successive layers of the target. At each layer the energy loss of the incident Nb ion was calculated, along with the probability that the Nb ion underwent a nuclear interaction, as calculated using an energy-dependent geometric cross section [20,21,22]. Then, a Monte-Carlo simulation determined whether or not the Nb ion underwent a nuclear interaction; if so, the Nb energy at which the interaction took place was noted, and the Monte Carlo simulation used the neutron cross section calculated for that Nb energy to generate the multiplicity of neutrons resulting from the interaction, as well as the distribution of neutron energies and angles.

As a matter of practicality, BUU calculations of the cross sections were done at a few selected energies, and each calculation was used to represent the production cross sections for a range of Nb energies; for example, BUU calculations were run at 50, 100, 150, 200, 250, 300, 350, and 400 MeV/nucleon Nb energies in order to compare with the 435 MeV/nucleon data. The cross sections calculated at 50 MeV/nucleon were used to produce neutrons for any Nb ion up to 75 MeV/nucleon interacting in the target. The cross sections calculated at 100 MeV/nucleon were used whenever a Nb ion between 75 and 125 MeV/nucleon interacted in the target. Like the calculation done at 100 MeV/nucleon, all other calculations were used for a 50 MeV/nucleon-wide range of Nb interactions, except for the cross sections calculated at 400 MeV/nucleon, which were used for Nb interactions between 375 and 435 MeV/nucleon.

Once the appropriate neutron multiplicities, energies, and trajectories were determined, each neutron that was produced in the simulation was followed to see if it made it within the geometrical acceptance of any of the detectors used in the experiment. Neutron interactions in the target were neglected. A minimum of 10^7 Nb ions were transported through the target in each of the simulations. The simulated stopping-target yields were then normalized for the number of Nb ions and for the solid angle of the detector, allowing for a direct comparison with the experimental data.

The contribution to the neutron yield from interactions between secondary fragments and the target were estimated by allowing the incoming Nb ion to remain intact after an interaction, keeping the same energy it had at the time of the initial interaction. This "secondary" fragment was then transported through the rest of the target in the same manner as the original Nb ion. This method most likely overestimates the contribution from secondary fragments because it artificially regenerates the neutrons liberated in the initial interaction; however, including this estimate of the secondary component to the neutron flux increased the neutron yields by no more than 10 percent when compared to the flux calculated using primary interactions only.

In addition to producing protons and neutrons, the BUU calculation used here [23] also includes the production of deuterons. In all calculations an incompressibility modulus of $K = 200$ was used.

Shown in Figs. 4 - 6 are spectra from all three systems along with the results from BUU calculations (solid lines). In the 435 MeV/nucleon Nb + Nb system (Fig. 4), the BUU model calculations compare well with the data at 28° and 48°, both in magnitude and in shape. At 80°, the BUU calculations do a good job predicting the magnitude of the spectrum, although it appears that the model predicts a slightly steeper slope than is observed with the data. At 9° and 16° the model does a good job of reproducing the shape of the spectra, but overpredicts the yields by 30% in both cases. At 3° the calculation again does a good job of reproducing the shape of the spectrum, but now it underpredicts the yield by a factor of 2.4. In the 272 MeV/nucleon Nb + Nb system (Fig. 5) the model overlaps the data at 48° and 80°, matches the shape well but overpredicts the yield by 50% at 28°, overpredicts the yield by a factor of 1.75 at 16°, matches the data at 9°, and underpredicts the yield by a factor of 2.2 at 3°. In the 272 MeV/nucleon Nb + Al data (Fig. 6) the model predicts a yield that falls off faster than the data as the energy decreases from 100 to 20 MeV at 3°, 9°, and 16°. Above 100 MeV, the spectral shapes at those angles are reproduced by the model calculation, although the normalizations are incorrect. At 3°, the model underpredicts the data by a factor of 3.7; at 9°, the yield is underpredicted by a factor of 1.6; and at 16°, the model overpredicts the yield by about 20%. At larger angles, the model underpredicts the yield by factors of 1.6 at 28°, 2.1 at 48°, and 1.6 at 80°.

Shown in the energy-distribution plots in Fig. 7 (left-hand side) are comparisons with the data using BUU (solid line) calculations. The BUU calculation does well in reproducing the data at 435 MeV/nucleon. Integrating the BUU calculation over energy gives a total yield of 4.23 neutrons per incident ion, in close agreement with the experimental value of 4.45 neutrons per incident ion. The BUU calculation of the energy distribution in the 272 MeV/nucleon Nb + Al system reproduces the shape of the spectrum, but underestimates the yield. Integrating the BUU-generated energy distribution gives a total yield of 1.2 neutrons per incident ion, whereas the experimental value is 2.2 neutrons per incident ion. In the 272 MeV/nucleon Nb + Nb system, the BUU calculation overestimates the yield at energies below 100 MeV, and underestimates the yield above 400 MeV. Integrating the BUU calculation over energy gives a total yield of 2.09 neutrons per incident ion, while the experimental total yield is 1.68 neutrons per incident ion. The disagreement between the model and data in the 272 MeV/nucleon Nb + Nb system indicates that the good agreement in the 435 MeV/nucleon Nb + Nb system may be fortuitous. Because the model overpredicts the yield below 100 MeV for the 272 MeV/nucleon systems, it must underpredict that same yield for ion energies ranging between 272 and 435 MeV/nucleon in order to match the data from the 435 MeV/nucleon system.

The disagreement between the data and model predictions is great enough to warrant further study; however, at this point it cannot be said whether the disagreement lies with (1) the BUU calculations of the cross sections, or (2) the method of applying the BUU-generated cross sections to produce stopping-target yields. The very forward spectra (which are dominated by fragmentation processes and evaporation from the projectile-like remnant) that are calculated by BUU are sensitive to the cut-off density used in the calculation to determine whether a particle has been emitted or not. The value of the cut-off density used in the calculations here is 1/8 of normal nuclear density (taken to be 0.163 nucleons/fm^3). Using a cut-off density of 1/16 of normal nuclear density led to a 20% to 30% reduction in the yields at 3° and 9°, whereas it led to less than a 10% reduction in the yields at larger angles. Although the change in the magnitude of the yield

at forward angles is significant when the cutoff density is reduced by a factor of two, the change is not enough to reproduce the data at forward angles.

As noted above, the BUU model used here also produces deuterons. The inclusion of complex-particle formation into BUU-model calculations has led to better comparisons between model calculations and cross section data; however, in order to compare model calculations with stopping-target data, complex particles formed in the calculation should be followed as they are transported through the remainder of the target to see if they undergo a nuclear interaction that produces neutron(s). That step was not taken in the comparisons shown here, which may be one reason why the calculations underestimate the yield at forward angles.

No firm conclusions can be drawn here in regards to the disagreement between the data and the BUU calculations because all or part of the disagreement may lie with the method that used the BUU calculations to produce stopping-target data. The BUU calculations will need to be compared directly to cross section data in order to firmly establish any shortcomings of using BUU-generated spectra in the method used here.

VI. CONCLUSIONS

Neutron angular and energy distributions, angle-integrated distributions, and energy-integrated distributions were measured for 272 and 435 MeV/nucleon Nb + Nb, and 272 MeV/nucleon Nb + Al interactions in stopping targets. Neutrons were measured from 20 MeV up to energies of twice the beam energy per nucleon. In all three systems contributions from projectile fragmentation can be seen as broad bumps in the forward-angle spectra. Spectra at larger angles obey an exponential behavior seen in similar thin-target experiments. The energy distributions in all three systems fall off with increasing neutron energy. The total yields (integrated from 20 MeV on up and integrated from 0° to 90°) are 4.45 neutrons per incident ion in the 435 MeV/nucleon system, 1.68 neutrons per incident ion in the 272 MeV/nucleon Nb + Nb system, and 2.18 neutrons per incident ion in the 272 MeV/nucleon Nb + Al system. To first order, the total yields scale with the estimated fraction of interactions by the projectile in the stopping target and the number of neutrons in the projectile-target system; however, data below 20 MeV will be needed to draw a firm mathematical relationship between the total yield and the fraction of Nb - target interactions, along with the number of neutrons in those systems. From these data, the ratio of the total yields in the two 272 MeV/nucleon systems is given by the ratio of the interaction fraction seen in the two systems weighted by the number of neutrons in the two systems, if half of the target neutrons and all of the projectile neutrons are used to calculate the number of participating neutrons in each system. BUU model calculations did well in reproducing the large-angle data in the Nb + Nb systems. In the forward-angle Nb + Nb data and in the Nb + Al data, BUU calculations in general reproduced the spectral shapes, but either underpredicted or overpredicted the yield, depending on angle and system.

ACKNOWLEDGMENTS

This work was supported in part by the National Science Foundation under Grants Nos. PHY-96-05207, PHY-91-07064, PHY-88-02392, and PHY-86-11210, the U.S. Department of Energy under Grants Nos. DE-FG89ER40531 and DE-AC03-76SF00098, and the National Aeronautics and Space Administration under NASA Grant L14230C.

Present addresses:

(α) Southern University, New Orleans, La.

(β) CyberAccess, Inc., Valley View, OH 44125

(γ) Picker International, Solon, OH

(δ) Dept. of Physics, U. of Wisconsin-Stout, Menomonie, WI

(ϵ) Crump Institute for Biological Imaging, UCLA, Los Angeles, CA 90095-6948

(ζ) Department of Chemistry, Texas A&M University, College Station, TX 77843

REFERENCES

1. L. C. Simonsen and J. E. Nealy, NASA Technical Paper 3079, (1991)

2. ICRP Publication 60 "Annals of the ICRP - 1990 Recommendations of the International Commission on Radiation Protection", Vol. 21, No. 1-3, Pergamon Press, Oxford, U.K. (1990)

3. NCRP Report No. 98 "Guidance on Radiation Received in Space Activites", National Council on Radiation Protection and Measurements, NCRP Publications, Bethesda, Md. (1989)

4. F. A. Cucinotta, NASA Technical Paper 3354, November 1993

5. J. W. Wilson, L. W. Townsend, W. Schimmerling, G. S. Khandelwal, F. Khan, J. E. Nealy, F. A. Cucinotta, L. C. Simonsen, J. L. Shinn, and J. W. Norbury, NASA Reference Publication 1257, (1991)

6. A. R. Baldwin, R. Madey, W.-M. Zhang, B. D. Anderson, D. Keane, J. Varga, J. W. Watson, G. D. Westfall, K. Frankel, and C. Gale, Phys. Rev. C **46**, 258, (1992)

7. W. Schimmerling, J. W. Kast, D. Ortendahl, R. Madey, R. A. Cecil, B. D. Anderson, and A. R. Baldwin, Phys. Rev. Lett. **43**, 1985, (1979)

8. R. A. Cecil, B. D. Anderson, A. R. Baldwin, R. Madey, W. Schimmerling, J. W. Kast, and D. Ortendahl, Phys. Rev. C **24**, 2013 (1981)

9. R. Madey, J. Varga, A. R. Baldwin, B. D. Anderson, R. A. Cecil, G. Fai, P. C. Tandy, J. W. Watson, and G. D. Westfall, Phys. Rev. Lett **55**, 1453, (1985)

10. R. Madey, B. D. Anderson, R. A. Cecil, P. C. Tandy, and W. Schimmerling, Phys. Rev. C **28**, 706 (1983)

11. R. Madey, W. M. Zhang, B. D. Anderson, A. R. Baldwin, M. Elaasar, B. S. Flanders, D. Keane, W. Pairsuwan, J. Varga, J. W. Watson, G. D. Westfall, C. Hartnack, H. Stocker, and K. Frankel, Phys. Rev. C **42**, 1068 (1990)

12. R. A. Cecil, B. D. Anderson, A. R. Baldwin, R. Madey, A. Galonsky, P. Miller, L. Young, and F. M. Waterman, Phys. Rev. C **21**, 2471, (1980)

13. M. M. Htun, R. Madey, W. M. Zhang, M. Elassar, D. Keane, B. D. Anderson, A. R. Baldwin, J. Jiang, A. Scott, Y. Shao, J. W. Watson, K. Frankel, L. Heilbronn, G. Krebs, M. A. McMahan, W. Rathbun, J. Schambach, G. D. Westfall, S. Yennello, C. Gale, and J. Zhang, Submitted to Phys. Rev. C, 1998.

14. A. R. Baldwin and R. Madey, Nucl. Inst. & Methods **161**, 439 (1980).

15. R. A. Cecil, B. D. Anderson, and R. Madey, Nucl. Instrum. Methods **161**, 439 (1979)

16. R. Serber, Phys. Rev. **72**, 10088 (1947)

17. A. S. Goldhaber, Phys. Lett. **53B**, 306 (1974)

18. R. Madey, W-M Zhang, B. D. Anderson, A. R. Baldwin, B. S. Flanders, W. Pairsuwan, J. Varga, J. W. Watson and G. D. Westfall, Phys. Rev. C **38**, 184 (1988)

19. Z. Chen, C. K. Gelbke, W. G. Gong, Y. D. Kim, W. G. Lynch, M. R. Maier, F. Saint-Laurent, D. Ardouin, H. Delagrange, H. Doubre, J. Kasagi, A. Kyanowski, A. Peghaire, J. Peter, E. Rosato, G. Bizard, F. Lefebvres, B. Tamain, J. Quebert, and Y. P. Viyogi, Phys. Rev. C **36**, 2297 (1987)

20. W. G. Gong, Ph.D. Thesis, Michigan State University (1992)

21. S. Kox, A. Gamp, C. Perrin, J. Arvieux, R. Bertholet, J. F. Bruandet, M. Buenerd, R. Cherkaoui, A. J. Cole, Y. El-Masri, N. Longequeue, J. Menet, F. Merchez, and J. B. Viano, Phys. Rev. C **35**, 1678 (1987)

22. L. W. Townsend and J. W. Wilson, Phys. Rev. C **37**, 892 (1988)

23. P. Danielewicz and G. F. Bertsch, Nucl. Phys. **A533**, 712 (1991)

LIST OF FIGURES

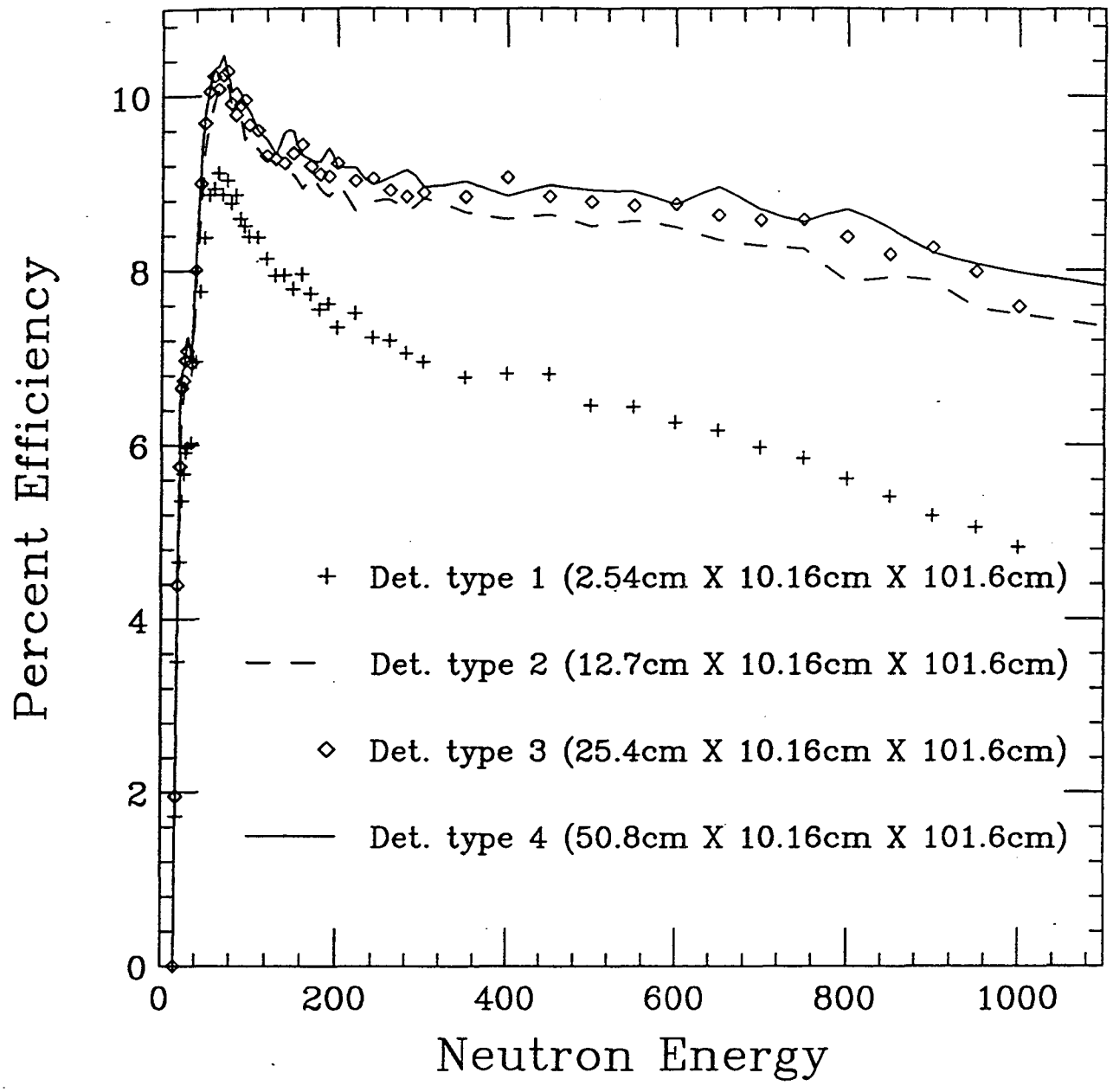

Fig. 1 - Neutron detection efficiency for all four sizes of detectors used in the experiment. Efficiencies shown here were calculated using a pulse-height threshold of 10 MeV equivalent electron energy.

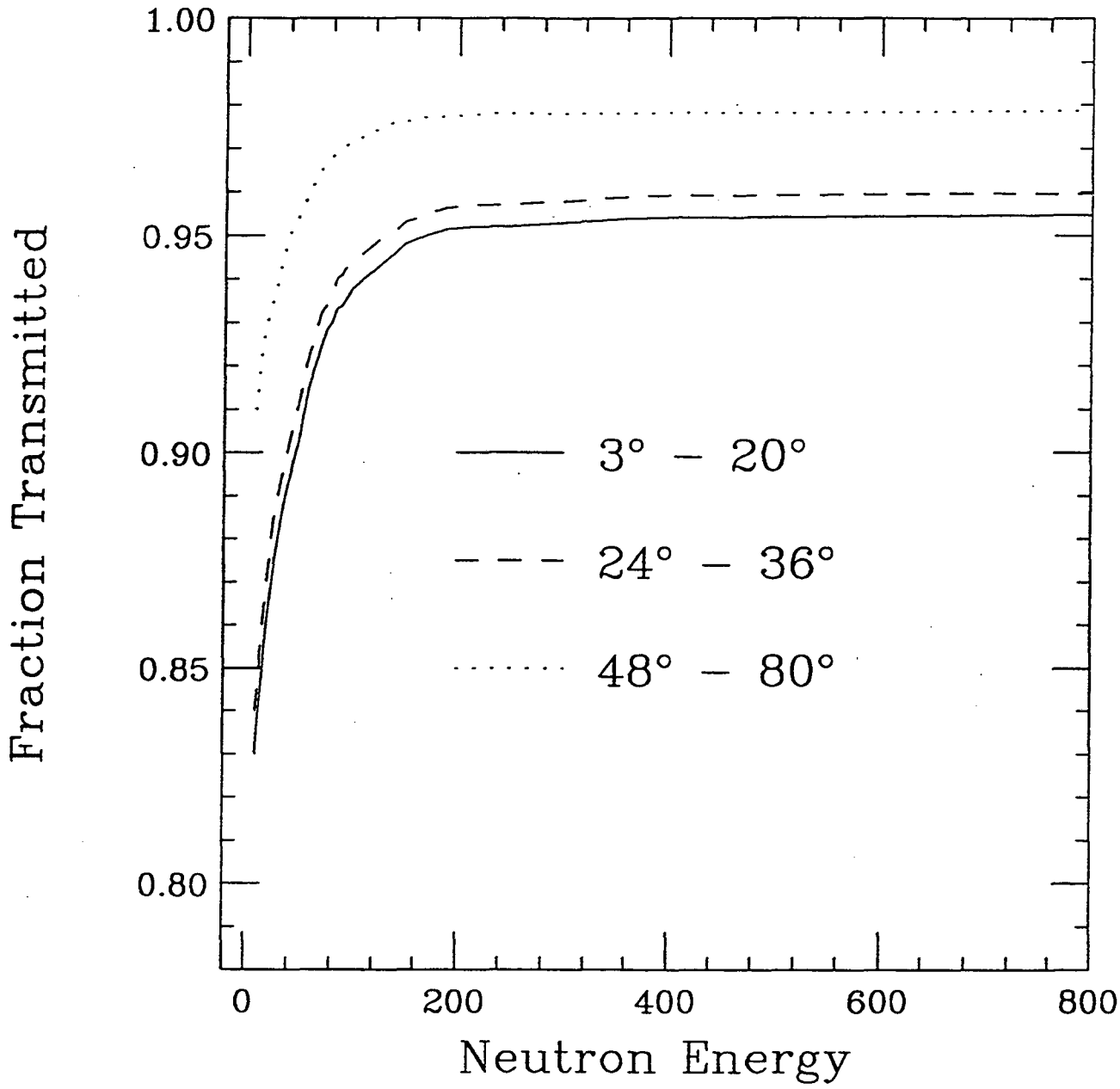

Fig. 2 - Fraction of the neutron flux transmitted from the target to the neutron detector as a function of neutron energy. The solid line shows the transmitted fraction for detectors between 3° and 20°, the dashed line is for detectors between 24° and 36°, and the dotted line is for detectors between 48° and 80°.

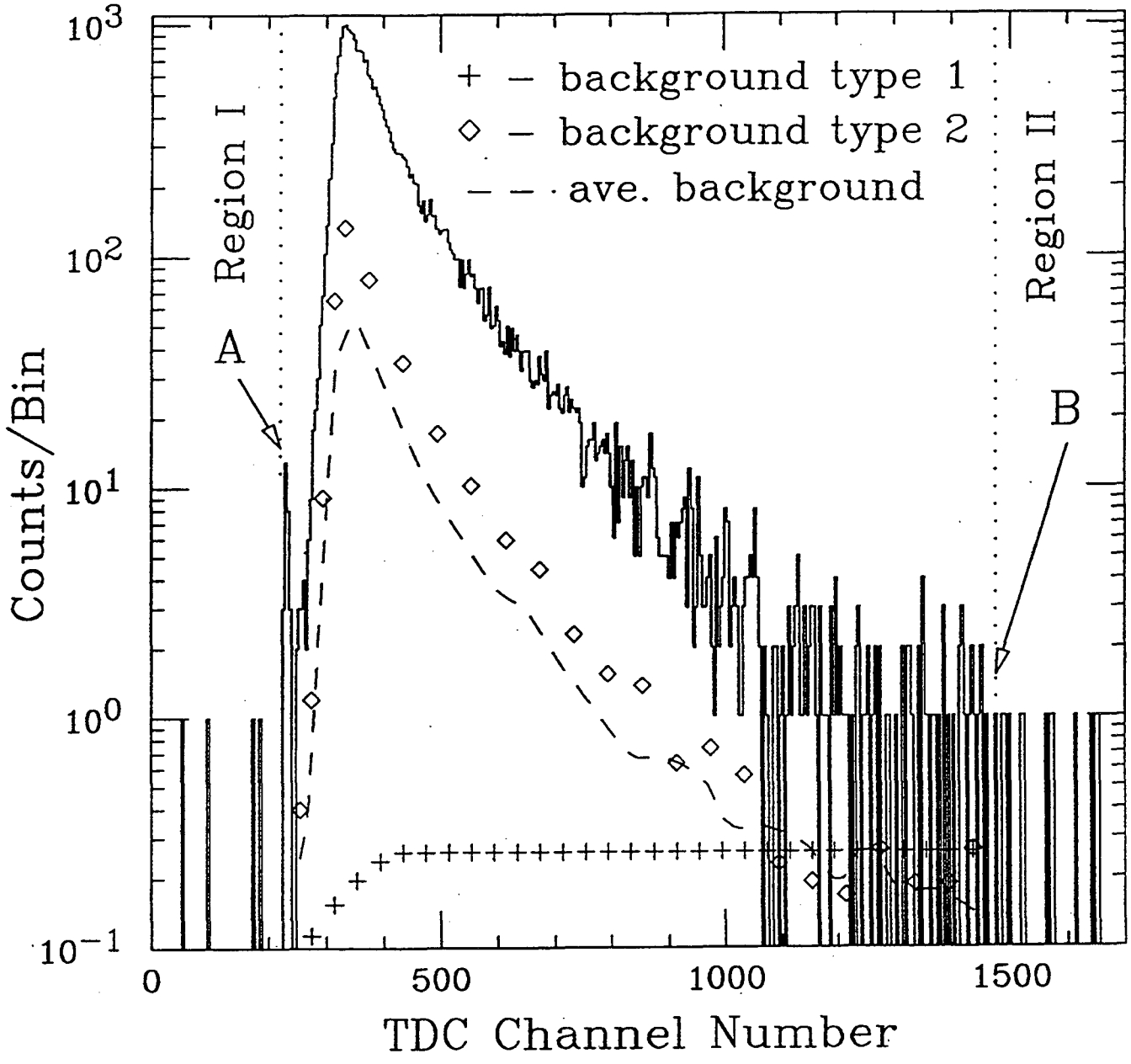

Fig. 3 - TDC spectrum at 3° from the 435 MeV/nucleon Nb + Nb system, for a pulse height threshold of 8 MeV equivalent electron energy. The peak labeled "A" is due to prompt gamma rays. The other labels delineate regions used to determine the background, as explained in the text.

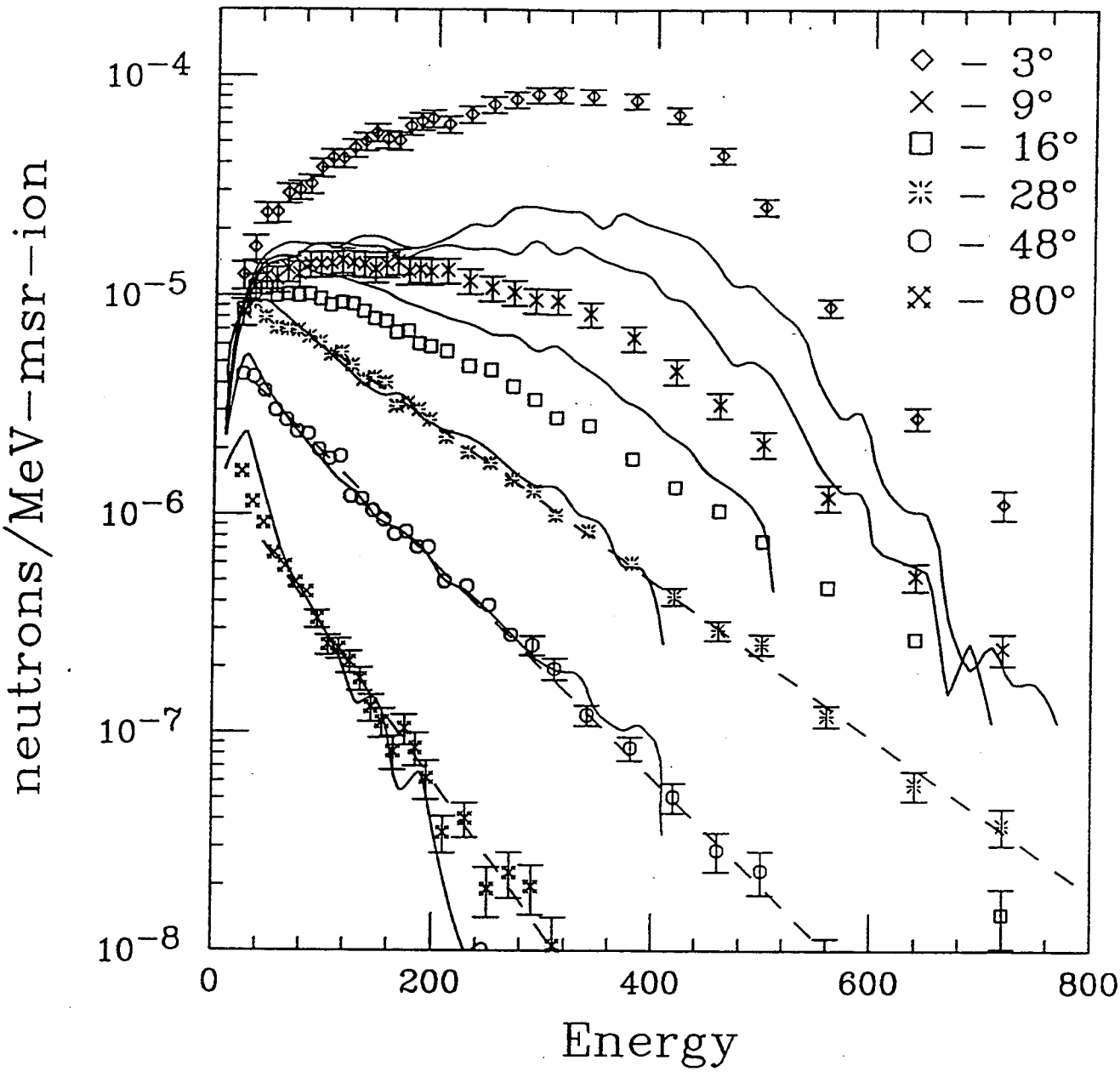

Fig. 4 - Neutron energy spectra from the 435 MeV/nucleon Nb + Nb system at 3°, 9°, 16°, 28°, 48°, and 80°. The data are shown with the symbols indicated in the plot. The solid lines are a fit to the data detailed in section V, and the dashed lines come from a fit to the data using Eqn. 1. Error bars have been suppressed where the plotted size of the uncertainty is less than the size of the plotting symbol.

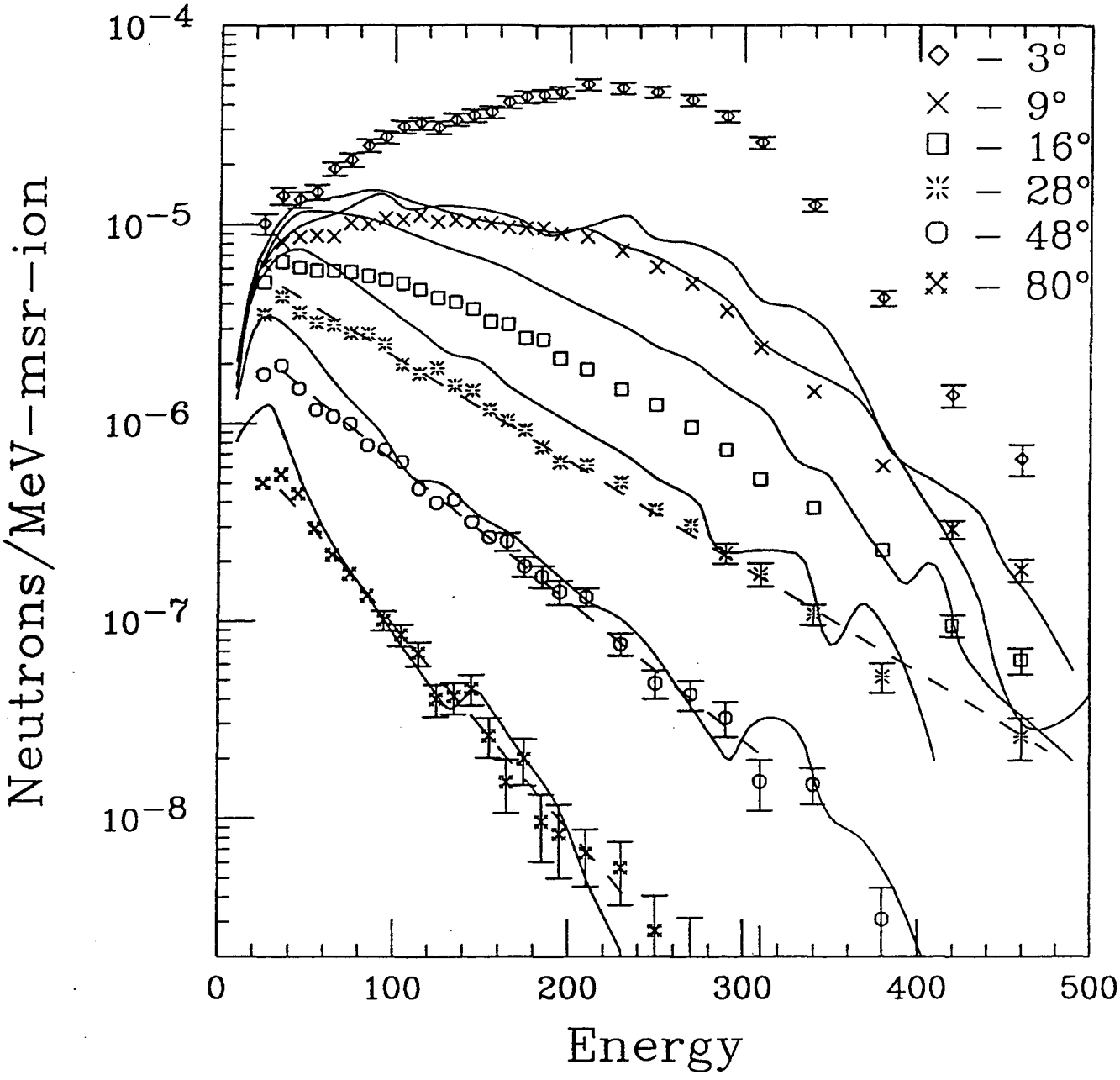

Fig. 5 - Neutron energy spectra from the 272 MeV/nucleon Nb + Nb system at 3°, 9°, 16°, 28
48°, and 80°. The data are shown with the symbols indicated in the plot. The solid lines are a
fit to the data detailed in section V, and the dashed lines come from a fit to the data using Eq
1. Error bars have been suppressed where the plotted size of the uncertainty is less than the si
of the plotting symbol.

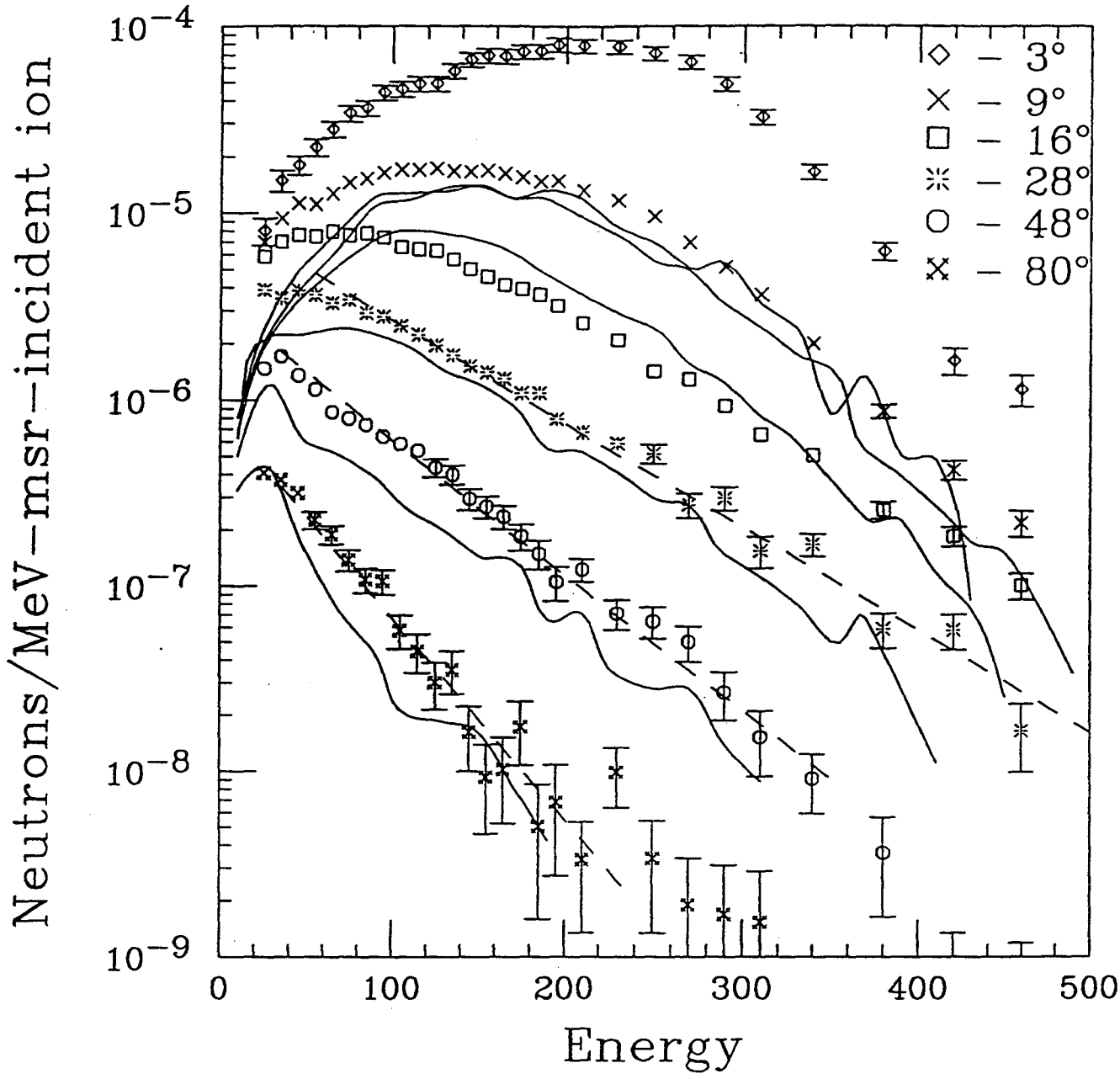

Fig. 6 - Neutron energy spectra from the 272 MeV/nucleon Nb + Al system at 3°, 9°, 16°, 28°, 48°, and 80°. The data are shown with the symbols indicated in the plot. The solid lines are a fit to the data detailed in section V, and the dashed lines come from a fit to the data using Eqn. 1. Error bars have been suppressed where the plotted size of the uncertainty is less than the size of the plotting symbol.

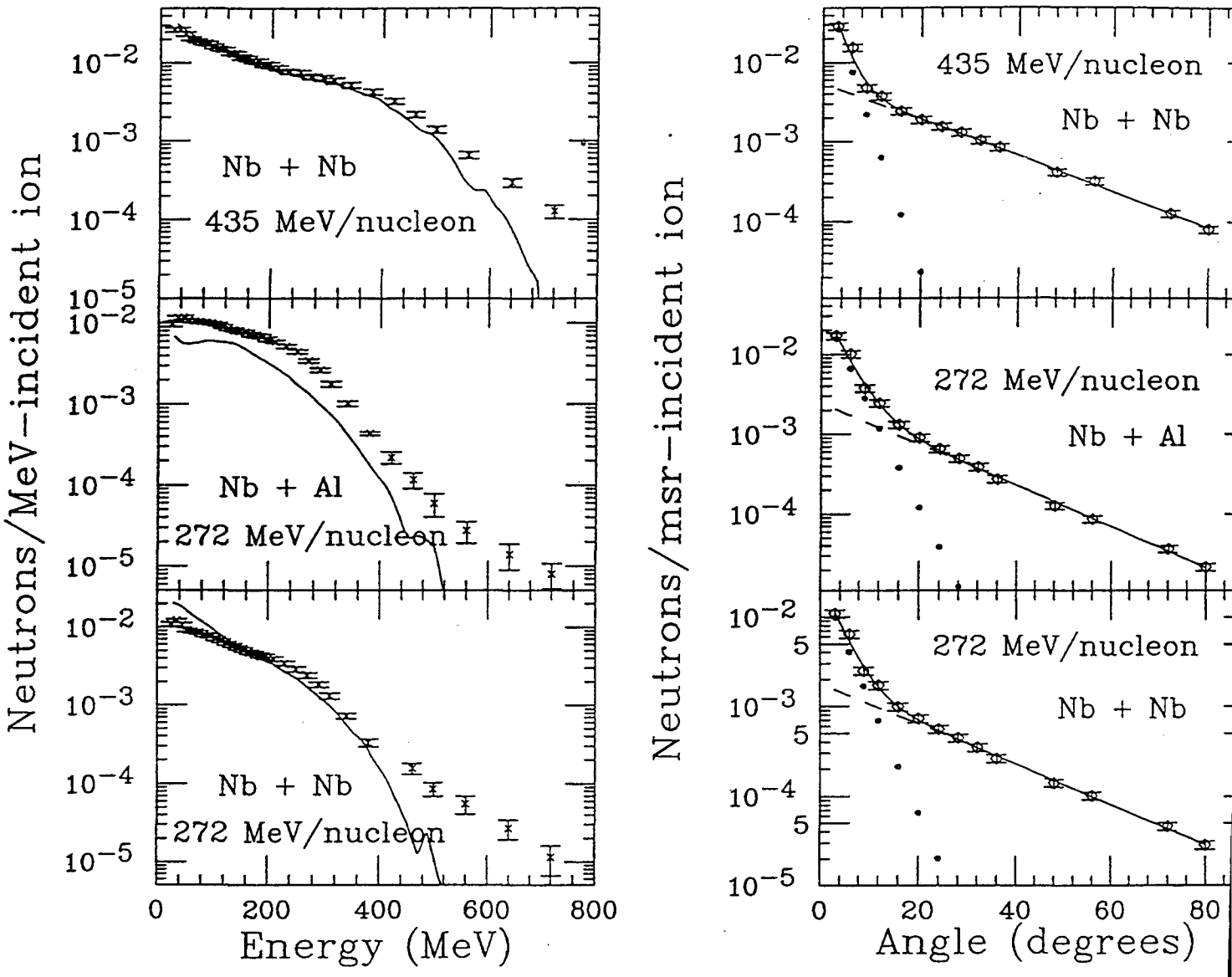

Fig. 7 - The plots on the left side show the neutron energy distributions from the systems indicated in each plot. The solid lines in the left-hand plots show a fit to the data using a method described in section V. The plots on the right side show the angular distributions from all three systems. The solid lines in the right-hand plots show a fit to the data using Equation 2 of the text. The dotted and dashed lines show the contributions from each component of Equation 2.

Energy (MeV)	Yield (n/MeV-msr-ion)
	3°
25.000	0.124E-04 ± 0.180E-05
35.000	0.165E-04 ± 0.207E-05
45.000	0.236E-04 ± 0.254E-05
55.000	0.238E-04 ± 0.248E-05
65.000	0.290E-04 ± 0.289E-05
75.000	0.300E-04 ± 0.297E-05
85.000	0.319E-04 ± 0.313E-05
95.000	0.379E-04 ± 0.363E-05
105.000	0.419E-04 ± 0.396E-05
115.000	0.417E-04 ± 0.395E-05
125.000	0.465E-04 ± 0.436E-05
135.000	0.499E-04 ± 0.464E-05
145.000	0.547E-04 ± 0.503E-05
155.000	0.510E-04 ± 0.473E-05
165.000	0.502E-04 ± 0.467E-05
175.000	0.585E-04 ± 0.535E-05
185.000	0.617E-04 ± 0.561E-05
195.000	0.634E-04 ± 0.576E-05
210.000	0.597E-04 ± 0.512E-05
230.000	0.663E-04 ± 0.566E-05
250.000	0.732E-04 ± 0.621E-05
270.000	0.773E-04 ± 0.655E-05
290.000	0.815E-04 ± 0.689E-05
310.000	0.820E-04 ± 0.693E-05
340.000	0.803E-04 ± 0.661E-05
380.000	0.766E-04 ± 0.631E-05
420.000	0.661E-04 ± 0.547E-05
460.000	0.432E-04 ± 0.365E-05
500.000	0.253E-04 ± 0.222E-05
560.000	0.884E-05 ± 0.808E-06
640.000	0.277E-05 ± 0.314E-06
720.000	0.112E-05 ± 0.170E-06
800.000	0.513E-06 ± 0.109E-06
880.000	0.267E-06 ± 0.779E-07
960.000	0.135E-06 ± 0.561E-07

Table A-I. Neutron yields from 435 MeV/nucleon Niobium stopping in a Niobium target. Yields are for the laboratory angle indicated in the table.

Energy (MeV)	Yield (n/MeV-msr-ion)
	6°
25.000	0.155E-04 ± 0.195E-05
35.000	0.237E-04 ± 0.239E-05
45.000	0.257E-04 ± 0.236E-05
55.000	0.304E-04 ± 0.258E-05
65.000	0.300E-04 ± 0.253E-05
75.000	0.332E-04 ± 0.274E-05
85.000	0.342E-04 ± 0.281E-05
95.000	0.347E-04 ± 0.286E-05
105.000	0.387E-04 ± 0.312E-05
115.000	0.409E-04 ± 0.327E-05
125.000	0.379E-04 ± 0.310E-05
135.000	0.453E-04 ± 0.357E-05
145.000	0.412E-04 ± 0.331E-05
155.000	0.419E-04 ± 0.336E-05
165.000	0.442E-04 ± 0.350E-05
175.000	0.443E-04 ± 0.353E-05
185.000	0.425E-04 ± 0.342E-05
195.000	0.444E-04 ± 0.355E-05
210.000	0.446E-04 ± 0.316E-05
230.000	0.372E-04 ± 0.271E-05
250.000	0.422E-04 ± 0.303E-05
270.000	0.385E-04 ± 0.281E-05
290.000	0.390E-04 ± 0.285E-05
310.000	0.372E-04 ± 0.274E-05
340.000	0.331E-04 ± 0.226E-05
380.000	0.265E-04 ± 0.186E-05
420.000	0.180E-04 ± 0.133E-05
460.000	0.115E-04 ± 0.934E-06
500.000	0.683E-05 ± 0.639E-06
560.000	0.254E-05 ± 0.262E-06
640.000	0.103E-05 ± 0.150E-06
720.000	0.381E-06 ± 0.881E-07
800.000	0.183E-06 ± 0.612E-07
880.000	0.921E-07 ± 0.445E-07
960.000	0.170E-08 ± 0.549E-08

Table A-I. Continued - caption on first page of table.

Energy (MeV)	Yield (n/MeV-msr-ion)
	9°
25.000	0.841E-05 ± 0.118E-05
35.000	0.109E-04 ± 0.148E-05
45.000	0.122E-04 ± 0.162E-05
55.000	0.118E-04 ± 0.157E-05
65.000	0.132E-04 ± 0.175E-05
75.000	0.125E-04 ± 0.166E-05
85.000	0.138E-04 ± 0.181E-05
95.000	0.138E-04 ± 0.181E-05
105.000	0.139E-04 ± 0.183E-05
115.000	0.144E-04 ± 0.190E-05
125.000	0.140E-04 ± 0.185E-05
135.000	0.138E-04 ± 0.182E-05
145.000	0.131E-04 ± 0.174E-05
155.000	0.138E-04 ± 0.182E-05
165.000	0.142E-04 ± 0.187E-05
175.000	0.128E-04 ± 0.170E-05
185.000	0.131E-04 ± 0.173E-05
195.000	0.128E-04 ± 0.169E-05
210.000	0.130E-04 ± 0.168E-05
230.000	0.116E-04 ± 0.151E-05
250.000	0.108E-04 ± 0.141E-05
270.000	0.103E-04 ± 0.135E-05
290.000	0.950E-05 ± 0.124E-05
310.000	0.941E-05 ± 0.123E-05
340.000	0.822E-05 ± 0.106E-05
380.000	0.640E-05 ± 0.831E-06
420.000	0.452E-05 ± 0.593E-06
460.000	0.317E-05 ± 0.422E-06
500.000	0.211E-05 ± 0.287E-06
560.000	0.120E-05 ± 0.162E-06
640.000	0.523E-06 ± 0.759E-07
720.000	0.244E-06 ± 0.402E-07
800.000	0.152E-06 ± 0.282E-07
880.000	0.706E-07 ± 0.167E-07
960.000	0.334E-07 ± 0.107E-07

Table A-I. Continued - caption on first page of table.

Energy (MeV)	Yield (n/MeV-msr-ion)
	12°
25.000	0.868E-05 ± 0.694E-06
35.000	0.121E-04 ± 0.855E-06
45.000	0.137E-04 ± 0.905E-06
55.000	0.130E-04 ± 0.850E-06
65.000	0.121E-04 ± 0.793E-06
75.000	0.128E-04 ± 0.828E-06
85.000	0.122E-04 ± 0.803E-06
95.000	0.124E-04 ± 0.812E-06
105.000	0.114E-04 ± 0.762E-06
115.000	0.119E-04 ± 0.789E-06
125.000	0.117E-04 ± 0.778E-06
135.000	0.113E-04 ± 0.757E-06
145.000	0.107E-04 ± 0.729E-06
155.000	0.116E-04 ± 0.781E-06
165.000	0.101E-04 ± 0.697E-06
175.000	0.958E-05 ± 0.668E-06
185.000	0.105E-04 ± 0.722E-06
195.000	0.915E-05 ± 0.646E-06
210.000	0.925E-05 ± 0.575E-06
230.000	0.848E-05 ± 0.535E-06
250.000	0.792E-05 ± 0.505E-06
270.000	0.699E-05 ± 0.455E-06
290.000	0.642E-05 ± 0.424E-06
310.000	0.592E-05 ± 0.397E-06
340.000	0.534E-05 ± 0.326E-06
380.000	0.386E-05 ± 0.248E-06
420.000	0.311E-05 ± 0.207E-06
460.000	0.227E-05 ± 0.162E-06
500.000	0.172E-05 ± 0.131E-06
560.000	0.984E-06 ± 0.726E-07
640.000	0.487E-06 ± 0.443E-07
720.000	0.208E-06 ± 0.262E-07
800.000	0.149E-06 ± 0.220E-07
880.000	0.685E-07 ± 0.145E-07
960.000	0.319E-07 ± 0.985E-08

Table A-I. Continued - caption on first page of table.

Energy (MeV)	Yield (n/MeV-msr-ion)
	16°
25.000	0.865E-05 ± 0.540E-06
35.000	0.108E-04 ± 0.626E-06
45.000	0.107E-04 ± 0.597E-06
55.000	0.997E-05 ± 0.553E-06
65.000	0.101E-04 ± 0.559E-06
75.000	0.996E-05 ± 0.550E-06
85.000	0.101E-04 ± 0.557E-06
95.000	0.962E-05 ± 0.535E-06
105.000	0.902E-05 ± 0.509E-06
115.000	0.926E-05 ± 0.522E-06
125.000	0.910E-05 ± 0.515E-06
135.000	0.845E-05 ± 0.485E-06
145.000	0.784E-05 ± 0.455E-06
155.000	0.760E-05 ± 0.443E-06
165.000	0.680E-05 ± 0.406E-06
175.000	0.690E-05 ± 0.412E-06
185.000	0.603E-05 ± 0.371E-06
195.000	0.585E-05 ± 0.361E-06
210.000	0.557E-05 ± 0.306E-06
230.000	0.476E-05 ± 0.269E-06
250.000	0.457E-05 ± 0.260E-06
270.000	0.384E-05 ± 0.226E-06
290.000	0.335E-05 ± 0.202E-06
310.000	0.277E-05 ± 0.174E-06
340.000	0.255E-05 ± 0.143E-06
380.000	0.180E-05 ± 0.107E-06
420.000	0.133E-05 ± 0.844E-07
460.000	0.104E-05 ± 0.702E-07
500.000	0.756E-06 ± 0.562E-07
560.000	0.464E-06 ± 0.325E-07
640.000	0.269E-06 ± 0.224E-07
720.000	0.147E-07 ± 0.444E-08

Table A-I. Continued - caption on first page of table.

Energy (MeV)	Yield (n/MeV-msr-ion)
	20°
25.000	0.750E-05 ± 0.526E-06
35.000	0.951E-05 ± 0.625E-06
45.000	0.897E-05 ± 0.575E-06
55.000	0.883E-05 ± 0.558E-06
65.000	0.852E-05 ± 0.539E-06
75.000	0.845E-05 ± 0.534E-06
85.000	0.823E-05 ± 0.524E-06
95.000	0.742E-05 ± 0.479E-06
105.000	0.778E-05 ± 0.501E-06
115.000	0.716E-05 ± 0.468E-06
125.000	0.693E-05 ± 0.456E-06
135.000	0.624E-05 ± 0.418E-06
145.000	0.616E-05 ± 0.413E-06
155.000	0.575E-05 ± 0.390E-06
165.000	0.517E-05 ± 0.358E-06
175.000	0.484E-05 ± 0.341E-06
185.000	0.436E-05 ± 0.315E-06
195.000	0.452E-05 ± 0.323E-06
210.000	0.389E-05 ± 0.252E-06
230.000	0.364E-05 ± 0.239E-06
250.000	0.323E-05 ± 0.216E-06
270.000	0.275E-05 ± 0.190E-06
290.000	0.240E-05 ± 0.170E-06
310.000	0.212E-05 ± 0.155E-06
340.000	0.169E-05 ± 0.112E-06
380.000	0.133E-05 ± 0.922E-07
420.000	0.914E-06 ± 0.688E-07
460.000	0.761E-06 ± 0.603E-07
500.000	0.499E-06 ± 0.448E-07
560.000	0.354E-06 ± 0.287E-07
640.000	0.183E-06 ± 0.183E-07
720.000	0.907E-07 ± 0.120E-07
800.000	0.593E-07 ± 0.947E-08
880.000	0.250E-07 ± 0.601E-08
960.000	0.625E-08 ± 0.300E-08

Table A-I. Continued - caption on first page of table.

Energy (MeV)	Yield (n/MeV-msr-ion)
	24°
25.000	0.703E-05 ± 0.445E-06
35.000	0.772E-05 ± 0.462E-06
45.000	0.801E-05 ± 0.453E-06
55.000	0.745E-05 ± 0.417E-06
65.000	0.684E-05 ± 0.387E-06
75.000	0.694E-05 ± 0.391E-06
85.000	0.734E-05 ± 0.411E-06
95.000	0.647E-05 ± 0.372E-06
105.000	0.649E-05 ± 0.374E-06
115.000	0.642E-05 ± 0.372E-06
125.000	0.598E-05 ± 0.354E-06
135.000	0.574E-05 ± 0.343E-06
145.000	0.500E-05 ± 0.309E-06
155.000	0.454E-05 ± 0.287E-06
165.000	0.416E-05 ± 0.269E-06
175.000	0.388E-05 ± 0.258E-06
185.000	0.331E-05 ± 0.231E-06
195.000	0.321E-05 ± 0.225E-06
210.000	0.293E-05 ± 0.175E-06
230.000	0.301E-05 ± 0.179E-06
250.000	0.257E-05 ± 0.159E-06
270.000	0.214E-05 ± 0.139E-06
290.000	0.173E-05 ± 0.120E-06
310.000	0.164E-05 ± 0.115E-06
340.000	0.132E-05 ± 0.813E-07
380.000	0.975E-06 ± 0.649E-07
420.000	0.749E-06 ± 0.541E-07
460.000	0.571E-06 ± 0.454E-07
500.000	0.420E-06 ± 0.375E-07
560.000	0.245E-06 ± 0.207E-07
640.000	0.140E-06 ± 0.147E-07
720.000	0.700E-07 ± 0.100E-07
800.000	0.348E-07 ± 0.698E-08
880.000	0.162E-07 ± 0.474E-08
960.000	0.765E-08 ± 0.330E-08

Table A-I. Continued - caption on first page of table.

Energy (MeV)	Yield (n/MeV-msr-ion)
	28°
25.000	0.832E-05 ± 0.512E-06
35.000	0.923E-05 ± 0.537E-06
45.000	0.793E-05 ± 0.455E-06
55.000	0.709E-05 ± 0.406E-06
65.000	0.698E-05 ± 0.398E-06
75.000	0.691E-05 ± 0.395E-06
85.000	0.646E-05 ± 0.376E-06
95.000	0.610E-05 ± 0.359E-06
105.000	0.537E-05 ± 0.327E-06
115.000	0.550E-05 ± 0.334E-06
125.000	0.481E-05 ± 0.304E-06
135.000	0.413E-05 ± 0.271E-06
145.000	0.423E-05 ± 0.276E-06
155.000	0.402E-05 ± 0.265E-06
165.000	0.313E-05 ± 0.222E-06
175.000	0.323E-05 ± 0.228E-06
185.000	0.302E-05 ± 0.218E-06
195.000	0.271E-05 ± 0.202E-06
210.000	0.226E-05 ± 0.145E-06
230.000	0.192E-05 ± 0.129E-06
250.000	0.172E-05 ± 0.120E-06
270.000	0.144E-05 ± 0.107E-06
290.000	0.128E-05 ± 0.983E-07
310.000	0.989E-06 ± 0.832E-07
340.000	0.840E-06 ± 0.592E-07
380.000	0.599E-06 ± 0.469E-07
420.000	0.422E-06 ± 0.374E-07
460.000	0.295E-06 ± 0.303E-07
500.000	0.255E-06 ± 0.279E-07
560.000	0.119E-06 ± 0.135E-07
640.000	0.576E-07 ± 0.900E-08
720.000	0.375E-07 ± 0.719E-08
800.000	0.191E-07 ± 0.511E-08
880.000	0.935E-08 ± 0.359E-08
960.000	0.564E-08 ± 0.282E-08

Table A-I. Continued - caption on first page of table.

Energy (MeV)	Yield (n/MeV-msr-ion)
	32°
25.000	0.757E-05 ± 0.508E-06
35.000	0.768E-05 ± 0.498E-06
45.000	0.602E-05 ± 0.393E-06
55.000	0.608E-05 ± 0.385E-06
65.000	0.535E-05 ± 0.346E-06
75.000	0.615E-05 ± 0.386E-06
85.000	0.532E-05 ± 0.346E-06
95.000	0.501E-05 ± 0.330E-06
105.000	0.440E-05 ± 0.300E-06
115.000	0.413E-05 ± 0.286E-06
125.000	0.373E-05 ± 0.266E-06
135.000	0.359E-05 ± 0.259E-06
145.000	0.314E-05 ± 0.234E-06
155.000	0.269E-05 ± 0.209E-06
165.000	0.252E-05 ± 0.201E-06
175.000	0.252E-05 ± 0.202E-06
185.000	0.222E-05 ± 0.185E-06
195.000	0.199E-05 ± 0.171E-06
210.000	0.176E-05 ± 0.128E-06
230.000	0.153E-05 ± 0.116E-06
250.000	0.123E-05 ± 0.994E-07
270.000	0.100E-05 ± 0.871E-07
290.000	0.990E-06 ± 0.863E-07
310.000	0.788E-06 ± 0.743E-07
340.000	0.652E-06 ± 0.520E-07
380.000	0.443E-06 ± 0.399E-07
420.000	0.338E-06 ± 0.336E-07
460.000	0.195E-06 ± 0.243E-07
500.000	0.154E-06 ± 0.212E-07
560.000	0.952E-07 ± 0.120E-07
640.000	0.498E-07 ± 0.840E-08
720.000	0.162E-07 ± 0.466E-08
800.000	0.112E-07 ± 0.390E-08
880.000	0.661E-08 ± 0.301E-08

Table A-I. Continued - caption on first page of table.

Energy (MeV)	Yield (n/MeV-msr-ion)
	36°
25.000	0.685E-05 ± 0.487E-06
35.000	0.668E-05 ± 0.464E-06
45.000	0.637E-05 ± 0.428E-06
55.000	0.555E-05 ± 0.374E-06
65.000	0.531E-05 ± 0.358E-06
75.000	0.458E-05 ± 0.318E-06
85.000	0.461E-05 ± 0.321E-06
95.000	0.423E-05 ± 0.300E-06
105.000	0.347E-05 ± 0.259E-06
115.000	0.330E-05 ± 0.250E-06
125.000	0.316E-05 ± 0.243E-06
135.000	0.295E-05 ± 0.232E-06
145.000	0.226E-05 ± 0.191E-06
155.000	0.199E-05 ± 0.174E-06
165.000	0.205E-05 ± 0.178E-06
175.000	0.209E-05 ± 0.182E-06
185.000	0.166E-05 ± 0.156E-06
195.000	0.144E-05 ± 0.142E-06
210.000	0.141E-05 ± 0.112E-06
230.000	0.980E-06 ± 0.872E-07
250.000	0.943E-06 ± 0.851E-07
270.000	0.763E-06 ± 0.742E-07
290.000	0.634E-06 ± 0.660E-07
310.000	0.542E-06 ± 0.598E-07
340.000	0.430E-06 ± 0.402E-07
380.000	0.318E-06 ± 0.329E-07
420.000	0.216E-06 ± 0.259E-07
460.000	0.152E-06 ± 0.212E-07
500.000	0.701E-07 ± 0.139E-07
560.000	0.643E-07 ± 0.969E-08
640.000	0.232E-07 ± 0.561E-08
720.000	0.122E-07 ± 0.403E-08
800.000	0.356E-08 ± 0.215E-08

Table A-I. Continued - caption on first page of table.

Energy (MeV)	Yield (n/MeV-msr-ion)
	48°
25.000	0.438E-05 ± 0.261E-06
35.000	0.427E-05 ± 0.250E-06
45.000	0.368E-05 ± 0.213E-06
55.000	0.300E-05 ± 0.177E-06
65.000	0.271E-05 ± 0.161E-06
75.000	0.240E-05 ± 0.147E-06
85.000	0.234E-05 ± 0.145E-06
95.000	0.199E-05 ± 0.128E-06
105.000	0.180E-05 ± 0.119E-06
115.000	0.185E-05 ± 0.122E-06
125.000	0.121E-05 ± 0.906E-07
135.000	0.118E-05 ± 0.892E-07
145.000	0.104E-05 ± 0.816E-07
155.000	0.949E-06 ± 0.768E-07
165.000	0.812E-06 ± 0.698E-07
175.000	0.834E-06 ± 0.711E-07
185.000	0.711E-06 ± 0.642E-07
195.000	0.710E-06 ± 0.641E-07
210.000	0.494E-06 ± 0.398E-07
230.000	0.470E-06 ± 0.387E-07
250.000	0.384E-06 ± 0.341E-07
270.000	0.281E-06 ± 0.280E-07
290.000	0.252E-06 ± 0.262E-07
310.000	0.196E-06 ± 0.227E-07
340.000	0.120E-06 ± 0.128E-07
380.000	0.848E-07 ± 0.105E-07
420.000	0.507E-07 ± 0.789E-08
460.000	0.288E-07 ± 0.581E-08
500.000	0.232E-07 ± 0.520E-08
560.000	0.906E-08 ± 0.229E-08
640.000	0.380E-08 ± 0.146E-08
720.000	0.344E-08 ± 0.141E-08

Table A-I. Continued - caption on first page of table.

Energy (MeV)	Yield (n/MeV-msr-ion)
	56°
25.000	0.442E-05 ± 0.248E-06
35.000	0.429E-05 ± 0.236E-06
45.000	0.328E-05 ± 0.182E-06
55.000	0.250E-05 ± 0.143E-06
65.000	0.227E-05 ± 0.132E-06
75.000	0.206E-05 ± 0.123E-06
85.000	0.180E-05 ± 0.112E-06
95.000	0.139E-05 ± 0.928E-07
105.000	0.139E-05 ± 0.930E-07
115.000	0.120E-05 ± 0.843E-07
125.000	0.947E-06 ± 0.723E-07
135.000	0.749E-06 ± 0.620E-07
145.000	0.726E-06 ± 0.604E-07
155.000	0.661E-06 ± 0.572E-07
165.000	0.615E-06 ± 0.551E-07
175.000	0.497E-06 ± 0.485E-07
185.000	0.397E-06 ± 0.423E-07
195.000	0.356E-06 ± 0.398E-07
210.000	0.321E-06 ± 0.284E-07
230.000	0.218E-06 ± 0.226E-07
250.000	0.180E-06 ± 0.202E-07
270.000	0.151E-06 ± 0.183E-07
290.000	0.107E-06 ± 0.151E-07
310.000	0.767E-07 ± 0.127E-07
340.000	0.446E-07 ± 0.687E-08
380.000	0.308E-07 ± 0.566E-08
420.000	0.193E-07 ± 0.444E-08
460.000	0.122E-07 ± 0.349E-08
500.000	0.538E-08 ± 0.230E-08
560.000	0.375E-08 ± 0.136E-08

Table A-I. Continued - caption on first page of table.

Energy (MeV)	Yield (n/MeV-msr-ion)
	72°
25.000	0.222E-05 ± 0.114E-06
35.000	0.181E-05 ± 0.951E-07
45.000	0.142E-05 ± 0.755E-07
55.000	0.117E-05 ± 0.636E-07
65.000	0.951E-06 ± 0.552E-07
75.000	0.739E-06 ± 0.473E-07
85.000	0.658E-06 ± 0.443E-07
95.000	0.601E-06 ± 0.423E-07
105.000	0.509E-06 ± 0.387E-07
115.000	0.391E-06 ± 0.335E-07
125.000	0.320E-06 ± 0.302E-07
135.000	0.288E-06 ± 0.284E-07
145.000	0.213E-06 ± 0.240E-07
155.000	0.225E-06 ± 0.249E-07
165.000	0.215E-06 ± 0.244E-07
175.000	0.140E-06 ± 0.195E-07
185.000	0.116E-06 ± 0.176E-07
195.000	0.119E-06 ± 0.179E-07
210.000	0.843E-07 ± 0.108E-07
230.000	0.499E-07 ± 0.825E-08
250.000	0.526E-07 ± 0.850E-08
270.000	0.251E-07 ± 0.579E-08
290.000	0.230E-07 ± 0.556E-08
310.000	0.116E-07 ± 0.395E-08
340.000	0.693E-08 ± 0.215E-08
380.000	0.526E-08 ± 0.188E-08
420.000	0.183E-08 ± 0.109E-08
460.000	0.162E-08 ± 0.102E-08

Table A-I. Continued - caption on first page of table.

Energy (MeV)	Yield (n/MeV-msr-ion)
	80°
25.000	0.157E-05 ± 0.100E-06
35.000	0.114E-05 ± 0.773E-07
45.000	0.912E-06 ± 0.618E-07
55.000	0.665E-06 ± 0.480E-07
65.000	0.578E-06 ± 0.433E-07
75.000	0.487E-06 ± 0.388E-07
85.000	0.441E-06 ± 0.366E-07
95.000	0.332E-06 ± 0.309E-07
105.000	0.253E-06 ± 0.265E-07
115.000	0.243E-06 ± 0.261E-07
125.000	0.211E-06 ± 0.242E-07
135.000	0.176E-06 ± 0.218E-07
145.000	0.130E-06 ± 0.183E-07
155.000	0.111E-06 ± 0.169E-07
165.000	0.815E-07 ± 0.144E-07
175.000	0.104E-06 ± 0.165E-07
185.000	0.847E-07 ± 0.147E-07
195.000	0.617E-07 ± 0.125E-07
210.000	0.347E-07 ± 0.666E-08
230.000	0.402E-07 ± 0.724E-08
250.000	0.191E-07 ± 0.493E-08
270.000	0.227E-07 ± 0.537E-08
290.000	0.196E-07 ± 0.499E-08
310.000	0.105E-07 ± 0.364E-08
340.000	0.709E-08 ± 0.211E-08
380.000	0.412E-08 ± 0.160E-08
420.000	0.488E-08 ± 0.176E-08
460.000	0.220E-08 ± 0.116E-08

Table A-I. Continued - caption on first page of table.

Energy (MeV)	Yield (n/MeV-msr-ion)
	3°
25.000	0.101E-04 ± 0.118E-05
35.000	0.139E-04 ± 0.136E-05
45.000	0.133E-04 ± 0.124E-05
55.000	0.145E-04 ± 0.126E-05
65.000	0.190E-04 ± 0.153E-05
75.000	0.210E-04 ± 0.165E-05
85.000	0.248E-04 ± 0.189E-05
95.000	0.274E-04 ± 0.205E-05
105.000	0.309E-04 ± 0.227E-05
115.000	0.322E-04 ± 0.236E-05
125.000	0.306E-04 ± 0.227E-05
135.000	0.335E-04 ± 0.245E-05
145.000	0.352E-04 ± 0.255E-05
155.000	0.366E-04 ± 0.263E-05
165.000	0.410E-04 ± 0.289E-05
175.000	0.435E-04 ± 0.305E-05
185.000	0.444E-04 ± 0.311E-05
195.000	0.461E-04 ± 0.322E-05
210.000	0.504E-04 ± 0.322E-05
230.000	0.482E-04 ± 0.309E-05
250.000	0.459E-04 ± 0.296E-05
270.000	0.420E-04 ± 0.274E-05
290.000	0.346E-04 ± 0.231E-05
310.000	0.255E-04 ± 0.177E-05
340.000	0.124E-04 ± 0.866E-06
380.000	0.424E-05 ± 0.375E-06
420.000	0.137E-05 ± 0.179E-06
460.000	0.654E-06 ± 0.117E-06
500.000	0.390E-06 ± 0.903E-07
560.000	0.220E-06 ± 0.484E-07
640.000	0.120E-06 ± 0.357E-07
720.000	0.414E-07 ± 0.211E-07

Table A-II. Neutron yields from 272 MeV/nucleon Niobium stopping in a Niobium target. Yields are for the laboratory angle indicated in the table.

Energy (MeV)	Yield (n/MeV-msr-ion)
	6°
25.000	0.979E-05 ± 0.111E-05
35.000	0.158E-04 ± 0.139E-05
45.000	0.170E-04 ± 0.135E-05
55.000	0.176E-04 ± 0.133E-05
65.000	0.193E-04 ± 0.140E-05
75.000	0.223E-04 ± 0.155E-05
85.000	0.236E-04 ± 0.162E-05
95.000	0.267E-04 ± 0.179E-05
105.000	0.254E-04 ± 0.173E-05
115.000	0.262E-04 ± 0.178E-05
125.000	0.280E-04 ± 0.188E-05
135.000	0.270E-04 ± 0.183E-05
145.000	0.262E-04 ± 0.180E-05
155.000	0.281E-04 ± 0.189E-05
165.000	0.258E-04 ± 0.177E-05
175.000	0.265E-04 ± 0.182E-05
185.000	0.260E-04 ± 0.180E-05
195.000	0.275E-04 ± 0.188E-05
210.000	0.261E-04 ± 0.155E-05
230.000	0.236E-04 ± 0.143E-05
250.000	0.198E-04 ± 0.125E-05
270.000	0.151E-04 ± 0.102E-05
290.000	0.981E-05 ± 0.754E-06
310.000	0.673E-05 ± 0.590E-06
340.000	0.267E-05 ± 0.256E-06
380.000	0.112E-05 ± 0.154E-06
420.000	0.332E-06 ± 0.802E-07
460.000	0.742E-07 ± 0.372E-07
500.000	0.710E-07 ± 0.372E-07
560.000	0.615E-07 ± 0.247E-07
640.000	0.561E-08 ± 0.678E-08

Table A-II. Continued - caption on first page of table.

Energy (MeV)	Yield (n/MeV-msr-ion)
	9°
25.000	0.629E-05 ± 0.375E-06
35.000	0.812E-05 ± 0.414E-06
45.000	0.863E-05 ± 0.399E-06
55.000	0.878E-05 ± 0.387E-06
65.000	0.870E-05 ± 0.379E-06
75.000	0.101E-04 ± 0.417E-06
85.000	0.100E-04 ± 0.419E-06
95.000	0.107E-04 ± 0.440E-06
105.000	0.106E-04 ± 0.439E-06
115.000	0.111E-04 ± 0.454E-06
125.000	0.103E-04 ± 0.434E-06
135.000	0.105E-04 ± 0.440E-06
145.000	0.102E-04 ± 0.431E-06
155.000	0.101E-04 ± 0.429E-06
165.000	0.964E-05 ± 0.416E-06
175.000	0.955E-05 ± 0.413E-06
185.000	0.958E-05 ± 0.416E-06
195.000	0.896E-05 ± 0.397E-06
210.000	0.864E-05 ± 0.318E-06
230.000	0.734E-05 ± 0.282E-06
250.000	0.607E-05 ± 0.246E-06
270.000	0.502E-05 ± 0.216E-06
290.000	0.366E-05 ± 0.175E-06
310.000	0.239E-05 ± 0.134E-06
340.000	0.144E-05 ± 0.752E-07
380.000	0.606E-06 ± 0.452E-07
420.000	0.289E-06 ± 0.302E-07
460.000	0.180E-06 ± 0.236E-07
500.000	0.640E-07 ± 0.139E-07
560.000	0.355E-07 ± 0.733E-08
640.000	0.119E-07 ± 0.423E-08

Table A-II. Continued - caption on first page of table.

Energy (MeV)	Yield (n/MeV-msr-ion)
	12°
25.000	0.635E-05 ± 0.387E-06
35.000	0.789E-05 ± 0.421E-06
45.000	0.836E-05 ± 0.409E-06
55.000	0.733E-05 ± 0.359E-06
65.000	0.775E-05 ± 0.368E-06
75.000	0.798E-05 ± 0.374E-06
85.000	0.781E-05 ± 0.371E-06
95.000	0.864E-05 ± 0.400E-06
105.000	0.778E-05 ± 0.372E-06
115.000	0.823E-05 ± 0.389E-06
125.000	0.731E-05 ± 0.359E-06
135.000	0.713E-05 ± 0.353E-06
145.000	0.663E-05 ± 0.337E-06
155.000	0.696E-05 ± 0.349E-06
165.000	0.627E-05 ± 0.326E-06
175.000	0.581E-05 ± 0.310E-06
185.000	0.537E-05 ± 0.296E-06
195.000	0.521E-05 ± 0.290E-06
210.000	0.438E-05 ± 0.206E-06
230.000	0.400E-05 ± 0.194E-06
250.000	0.306E-05 ± 0.162E-06
270.000	0.254E-05 ± 0.144E-06
290.000	0.194E-05 ± 0.121E-06
310.000	0.152E-05 ± 0.104E-06
340.000	0.903E-06 ± 0.581E-07
380.000	0.503E-06 ± 0.414E-07
420.000	0.262E-06 ± 0.289E-07
460.000	0.142E-06 ± 0.209E-07
500.000	0.115E-06 ± 0.188E-07
560.000	0.439E-07 ± 0.820E-08
640.000	0.158E-07 ± 0.492E-08

Table A-II. Continued - caption on first page of table.

Energy (MeV)	Yield (n/MeV-msr-ion)
	16°
25.000	0.516E-05 ± 0.251E-06
35.000	0.651E-05 ± 0.280E-06
45.000	0.610E-05 ± 0.251E-06
55.000	0.588E-05 ± 0.235E-06
65.000	0.587E-05 ± 0.233E-06
75.000	0.577E-05 ± 0.230E-06
85.000	0.553E-05 ± 0.225E-06
95.000	0.530E-05 ± 0.218E-06
105.000	0.508E-05 ± 0.212E-06
115.000	0.473E-05 ± 0.203E-06
125.000	0.429E-05 ± 0.191E-06
135.000	0.409E-05 ± 0.185E-06
145.000	0.376E-05 ± 0.175E-06
155.000	0.324E-05 ± 0.158E-06
165.000	0.315E-05 ± 0.156E-06
175.000	0.268E-05 ± 0.141E-06
185.000	0.264E-05 ± 0.140E-06
195.000	0.212E-05 ± 0.122E-06
210.000	0.187E-05 ± 0.874E-07
230.000	0.148E-05 ± 0.756E-07
250.000	0.123E-05 ± 0.673E-07
270.000	0.951E-06 ± 0.580E-07
290.000	0.731E-06 ± 0.498E-07
310.000	0.521E-06 ± 0.411E-07
340.000	0.374E-06 ± 0.252E-07
380.000	0.228E-06 ± 0.190E-07
420.000	0.946E-07 ± 0.119E-07
460.000	0.627E-07 ± 0.965E-08
500.000	0.359E-07 ± 0.727E-08
560.000	0.170E-07 ± 0.354E-08
640.000	0.746E-08 ± 0.234E-08
720.000	0.379E-08 ± 0.167E-08

Table A-II. Continued - caption on first page of table.

Energy (MeV)	Yield (n/MeV-msr-ion)
	20°
25.000	0.428E-05 ± 0.270E-06
35.000	0.500E-05 ± 0.295E-06
45.000	0.504E-05 ± 0.284E-06
55.000	0.454E-05 ± 0.254E-06
65.000	0.456E-05 ± 0.254E-06
75.000	0.445E-05 ± 0.249E-06
85.000	0.438E-05 ± 0.247E-06
95.000	0.404E-05 ± 0.231E-06
105.000	0.351E-05 ± 0.208E-06
115.000	0.341E-05 ± 0.204E-06
125.000	0.318E-05 ± 0.194E-06
135.000	0.275E-05 ± 0.174E-06
145.000	0.244E-05 ± 0.159E-06
155.000	0.245E-05 ± 0.159E-06
165.000	0.204E-05 ± 0.139E-06
175.000	0.186E-05 ± 0.131E-06
185.000	0.168E-05 ± 0.122E-06
195.000	0.142E-05 ± 0.109E-06
210.000	0.139E-05 ± 0.880E-07
230.000	0.946E-06 ± 0.666E-07
250.000	0.729E-06 ± 0.559E-07
270.000	0.619E-06 ± 0.504E-07
290.000	0.520E-06 ± 0.451E-07
310.000	0.379E-06 ± 0.371E-07
340.000	0.277E-06 ± 0.235E-07
380.000	0.177E-06 ± 0.177E-07
420.000	0.974E-07 ± 0.125E-07
460.000	0.563E-07 ± 0.934E-08
500.000	0.390E-07 ± 0.771E-08
560.000	0.140E-07 ± 0.324E-08
640.000	0.369E-08 ± 0.164E-08

Table A-II. Continued - caption on first page of table.

Energy (MeV)	Yield (n/MeV-msr-ion)
	24°
25.000	0.348E-05 ± 0.204E-06
35.000	0.389E-05 ± 0.209E-06
45.000	0.366E-05 ± 0.187E-06
55.000	0.349E-05 ± 0.174E-06
65.000	0.340E-05 ± 0.170E-06
75.000	0.344E-05 ± 0.171E-06
85.000	0.330E-05 ± 0.167E-06
95.000	0.307E-05 ± 0.159E-06
105.000	0.285E-05 ± 0.152E-06
115.000	0.252E-05 ± 0.141E-06
125.000	0.240E-05 ± 0.137E-06
135.000	0.213E-05 ± 0.127E-06
145.000	0.190E-05 ± 0.118E-06
155.000	0.169E-05 ± 0.110E-06
165.000	0.146E-05 ± 0.100E-06
175.000	0.140E-05 ± 0.984E-07
185.000	0.127E-05 ± 0.931E-07
195.000	0.113E-05 ± 0.867E-07
210.000	0.906E-06 ± 0.577E-07
230.000	0.694E-06 ± 0.492E-07
250.000	0.693E-06 ± 0.493E-07
270.000	0.407E-06 ± 0.364E-07
290.000	0.397E-06 ± 0.359E-07
310.000	0.316E-06 ± 0.316E-07
340.000	0.208E-06 ± 0.184E-07
380.000	0.148E-06 ± 0.152E-07
420.000	0.767E-07 ± 0.107E-07
460.000	0.415E-07 ± 0.782E-08
500.000	0.403E-07 ± 0.773E-08
560.000	0.168E-07 ± 0.353E-08
640.000	0.461E-08 ± 0.183E-08

Table A-II. Continued - caption on first page of table.

Energy (MeV)	Yield (n/MeV-msr-ion)
	28°
25.000	0.353E-05 ± 0.217E-06
35.000	0.435E-05 ± 0.240E-06
45.000	0.361E-05 ± 0.197E-06
55.000	0.321E-05 ± 0.175E-06
65.000	0.313E-05 ± 0.170E-06
75.000	0.284E-05 ± 0.158E-06
85.000	0.283E-05 ± 0.159E-06
95.000	0.251E-05 ± 0.146E-06
105.000	0.199E-05 ± 0.126E-06
115.000	0.178E-05 ± 0.117E-06
125.000	0.190E-05 ± 0.123E-06
135.000	0.155E-05 ± 0.108E-06
145.000	0.146E-05 ± 0.104E-06
155.000	0.117E-05 ± 0.904E-07
165.000	0.103E-05 ± 0.840E-07
175.000	0.921E-06 ± 0.790E-07
185.000	0.755E-06 ± 0.706E-07
195.000	0.635E-06 ± 0.637E-07
210.000	0.613E-06 ± 0.469E-07
230.000	0.500E-06 ± 0.416E-07
250.000	0.364E-06 ± 0.347E-07
270.000	0.304E-06 ± 0.315E-07
290.000	0.220E-06 ± 0.263E-07
310.000	0.172E-06 ± 0.230E-07
340.000	0.108E-06 ± 0.130E-07
380.000	0.518E-07 ± 0.876E-08
420.000	0.501E-07 ± 0.860E-08
460.000	0.257E-07 ± 0.613E-08
500.000	0.143E-07 ± 0.456E-08
560.000	0.847E-08 ± 0.249E-08
640.000	0.201E-08 ± 0.118E-08

Table A-II. Continued - caption on first page of table.

Energy (MeV)	Yield (n/MeV-msr-ion)
	32°
25.000	0.306E-05 ± 0.207E-06
35.000	0.313E-05 ± 0.203E-06
45.000	0.306E-05 ± 0.188E-06
55.000	0.273E-05 ± 0.167E-06
65.000	0.245E-05 ± 0.153E-06
75.000	0.245E-05 ± 0.153E-06
85.000	0.197E-05 ± 0.132E-06
95.000	0.182E-05 ± 0.125E-06
105.000	0.174E-05 ± 0.121E-06
115.000	0.148E-05 ± 0.109E-06
125.000	0.118E-05 ± 0.948E-07
135.000	0.988E-06 ± 0.850E-07
145.000	0.106E-05 ± 0.885E-07
155.000	0.876E-06 ± 0.784E-07
165.000	0.748E-06 ± 0.714E-07
175.000	0.648E-06 ± 0.661E-07
185.000	0.627E-06 ± 0.650E-07
195.000	0.508E-06 ± 0.573E-07
210.000	0.429E-06 ± 0.391E-07
230.000	0.381E-06 ± 0.365E-07
250.000	0.271E-06 ± 0.299E-07
270.000	0.265E-06 ± 0.297E-07
290.000	0.174E-06 ± 0.235E-07
310.000	0.145E-06 ± 0.212E-07
340.000	0.981E-07 ± 0.126E-07
380.000	0.492E-07 ± 0.860E-08
420.000	0.381E-07 ± 0.750E-08
460.000	0.199E-07 ± 0.540E-08
500.000	0.514E-08 ± 0.269E-08
560.000	0.522E-08 ± 0.194E-08
720.000	0.286E-08 ± 0.144E-08

Table A-II. Continued - caption on first page of table.

Energy (MeV)	Yield (n/MeV-msr-ion)
	36°
25.000	0.188E-05 ± 0.144E-06
35.000	0.262E-05 ± 0.170E-06
45.000	0.230E-05 ± 0.145E-06
55.000	0.194E-05 ± 0.124E-06
65.000	0.189E-05 ± 0.121E-06
75.000	0.184E-05 ± 0.119E-06
85.000	0.151E-05 ± 0.105E-06
95.000	0.126E-05 ± 0.935E-07
105.000	0.129E-05 ± 0.954E-07
115.000	0.127E-05 ± 0.954E-07
125.000	0.106E-05 ± 0.857E-07
135.000	0.905E-06 ± 0.782E-07
145.000	0.800E-06 ± 0.726E-07
155.000	0.629E-06 ± 0.629E-07
165.000	0.621E-06 ± 0.626E-07
175.000	0.577E-06 ± 0.606E-07
185.000	0.423E-06 ± 0.511E-07
195.000	0.433E-06 ± 0.516E-07
210.000	0.289E-06 ± 0.303E-07
230.000	0.323E-06 ± 0.324E-07
250.000	0.161E-06 ± 0.222E-07
270.000	0.163E-06 ± 0.224E-07
290.000	0.130E-06 ± 0.199E-07
310.000	0.715E-07 ± 0.145E-07
340.000	0.587E-07 ± 0.942E-08
380.000	0.218E-07 ± 0.559E-08
420.000	0.267E-07 ± 0.621E-08
460.000	0.108E-07 ± 0.395E-08
500.000	0.623E-08 ± 0.299E-08
560.000	0.897E-09 ± 0.748E-09
720.000	0.345E-10 ± 0.694E-10

Table A-II. Continued - caption on first page of table.

Energy (MeV)	Yield (n/MeV-msr-ion)
	48°
25.000	0.177E-05 ± 0.101E-06
35.000	0.196E-05 ± 0.106E-06
45.000	0.150E-05 ± 0.821E-07
55.000	0.117E-05 ± 0.665E-07
65.000	0.108E-05 ± 0.623E-07
75.000	0.993E-06 ± 0.589E-07
85.000	0.774E-06 ± 0.501E-07
95.000	0.736E-06 ± 0.488E-07
105.000	0.643E-06 ± 0.450E-07
115.000	0.468E-06 ± 0.373E-07
125.000	0.397E-06 ± 0.340E-07
135.000	0.411E-06 ± 0.346E-07
145.000	0.317E-06 ± 0.296E-07
155.000	0.265E-06 ± 0.269E-07
165.000	0.253E-06 ± 0.264E-07
175.000	0.189E-06 ± 0.225E-07
185.000	0.168E-06 ± 0.211E-07
195.000	0.140E-06 ± 0.191E-07
210.000	0.132E-06 ± 0.136E-07
230.000	0.762E-07 ± 0.101E-07
250.000	0.479E-07 ± 0.792E-08
270.000	0.421E-07 ± 0.737E-08
290.000	0.320E-07 ± 0.641E-08
310.000	0.153E-07 ± 0.441E-08
340.000	0.148E-07 ± 0.308E-08
380.000	0.309E-08 ± 0.137E-08
420.000	0.438E-08 ± 0.165E-08
460.000	0.475E-08 ± 0.173E-08
500.000	0.736E-10 ± 0.111E-09
560.000	0.879E-09 ± 0.506E-09
640.000	0.447E-09 ± 0.348E-09

Table A-II. Continued - caption on first page of table.

Energy (MeV)	Yield (n/MeV-msr-ion)
	56°
25.000	0.164E-05 ± 0.942E-07
35.000	0.146E-05 ± 0.837E-07
45.000	0.113E-05 ± 0.654E-07
55.000	0.870E-06 ± 0.528E-07
65.000	0.823E-06 ± 0.504E-07
75.000	0.685E-06 ± 0.446E-07
85.000	0.562E-06 ± 0.394E-07
95.000	0.529E-06 ± 0.381E-07
105.000	0.468E-06 ± 0.355E-07
115.000	0.363E-06 ± 0.306E-07
125.000	0.299E-06 ± 0.275E-07
135.000	0.224E-06 ± 0.232E-07
145.000	0.197E-06 ± 0.215E-07
155.000	0.136E-06 ± 0.176E-07
165.000	0.128E-06 ± 0.172E-07
175.000	0.129E-06 ± 0.173E-07
185.000	0.852E-07 ± 0.138E-07
195.000	0.687E-07 ± 0.124E-07
210.000	0.398E-07 ± 0.671E-08
230.000	0.335E-07 ± 0.616E-08
250.000	0.190E-07 ± 0.461E-08
270.000	0.184E-07 ± 0.452E-08
290.000	0.170E-07 ± 0.434E-08
310.000	0.968E-08 ± 0.327E-08
340.000	0.483E-08 ± 0.162E-08
380.000	0.442E-08 ± 0.156E-08
420.000	0.238E-08 ± 0.113E-08

Table A-II. Continued - caption on first page of table.

Energy (MeV)	Yield (n/MeV-msr-ion)
	72°
25.000	0.845E-06 ± 0.460E-07
35.000	0.790E-06 ± 0.427E-07
45.000	0.629E-06 ± 0.342E-07
55.000	0.459E-06 ± 0.271E-07
65.000	0.402E-06 ± 0.248E-07
75.000	0.285E-06 ± 0.205E-07
85.000	0.241E-06 ± 0.189E-07
95.000	0.175E-06 ± 0.160E-07
105.000	0.165E-06 ± 0.156E-07
115.000	0.151E-06 ± 0.151E-07
125.000	0.909E-07 ± 0.116E-07
135.000	0.773E-07 ± 0.107E-07
145.000	0.599E-07 ± 0.931E-08
155.000	0.501E-07 ± 0.855E-08
165.000	0.414E-07 ± 0.782E-08
175.000	0.248E-07 ± 0.605E-08
185.000	0.225E-07 ± 0.574E-08
195.000	0.169E-07 ± 0.498E-08
210.000	0.106E-07 ± 0.279E-08
230.000	0.731E-08 ± 0.233E-08
250.000	0.606E-08 ± 0.213E-08
270.000	0.255E-08 ± 0.136E-08

Table A-II. Continued - caption on first page of table.

Energy (MeV)	Yield (n/MeV-msr-ion)
	80°
25.000	0.500E-06 ± 0.342E-07
35.000	0.552E-06 ± 0.351E-07
45.000	0.440E-06 ± 0.280E-07
55.000	0.295E-06 ± 0.212E-07
65.000	0.216E-06 ± 0.175E-07
75.000	0.173E-06 ± 0.155E-07
85.000	0.134E-06 ± 0.136E-07
95.000	0.101E-06 ± 0.117E-07
105.000	0.853E-07 ± 0.108E-07
115.000	0.683E-07 ± 0.974E-08
125.000	0.399E-07 ± 0.742E-08
135.000	0.410E-07 ± 0.751E-08
145.000	0.450E-07 ± 0.782E-08
155.000	0.261E-07 ± 0.596E-08
165.000	0.152E-07 ± 0.456E-08
175.000	0.199E-07 ± 0.524E-08
185.000	0.961E-08 ± 0.360E-08
195.000	0.830E-08 ± 0.335E-08
210.000	0.665E-08 ± 0.213E-08
230.000	0.561E-08 ± 0.197E-08
250.000	0.270E-08 ± 0.135E-08
270.000	0.199E-08 ± 0.115E-08
290.000	0.193E-08 ± 0.113E-08

Table A-II. Continued - caption on first page of table.

Energy (MeV)	Yield (n/MeV-msr-ion)
	3°
25.000	0.804E-05 ± 0.133E-05
35.000	0.149E-04 ± 0.192E-05
45.000	0.180E-04 ± 0.206E-05
55.000	0.224E-04 ± 0.236E-05
65.000	0.280E-04 ± 0.280E-05
75.000	0.341E-04 ± 0.329E-05
85.000	0.364E-04 ± 0.349E-05
95.000	0.443E-04 ± 0.413E-05
105.000	0.462E-04 ± 0.429E-05
115.000	0.493E-04 ± 0.455E-05
125.000	0.494E-04 ± 0.457E-05
135.000	0.575E-04 ± 0.522E-05
145.000	0.661E-04 ± 0.592E-05
155.000	0.696E-04 ± 0.619E-05
165.000	0.690E-04 ± 0.615E-05
175.000	0.731E-04 ± 0.649E-05
185.000	0.737E-04 ± 0.655E-05
195.000	0.797E-04 ± 0.703E-05
210.000	0.787E-04 ± 0.660E-05
230.000	0.776E-04 ± 0.652E-05
250.000	0.714E-04 ± 0.603E-05
270.000	0.641E-04 ± 0.546E-05
290.000	0.490E-04 ± 0.426E-05
310.000	0.325E-04 ± 0.296E-05
340.000	0.165E-04 ± 0.150E-05
380.000	0.622E-05 ± 0.671E-06
420.000	0.161E-05 ± 0.264E-06
460.000	0.113E-05 ± 0.215E-06
500.000	0.444E-06 ± 0.129E-06
560.000	0.248E-06 ± 0.690E-07
640.000	0.531E-07 ± 0.312E-07

Table A-III. Neutron yields from 272 MeV/nucleon Niobium stopping in an Aluminum target. Yields are for the laboratory angle indicated in the table.

Energy (MeV)	Yield (n/MeV-msr-ion)
	6°
25.000	0.166E-04 ± 0.185E-05
35.000	0.221E-04 ± 0.201E-05
45.000	0.264E-04 ± 0.203E-05
55.000	0.276E-04 ± 0.197E-05
65.000	0.314E-04 ± 0.211E-05
75.000	0.338E-04 ± 0.221E-05
85.000	0.396E-04 ± 0.245E-05
95.000	0.397E-04 ± 0.248E-05
105.000	0.461E-04 ± 0.275E-05
115.000	0.450E-04 ± 0.272E-05
125.000	0.423E-04 ± 0.263E-05
135.000	0.420E-04 ± 0.263E-05
145.000	0.465E-04 ± 0.282E-05
155.000	0.487E-04 ± 0.290E-05
165.000	0.434E-04 ± 0.269E-05
175.000	0.444E-04 ± 0.276E-05
185.000	0.450E-04 ± 0.279E-05
195.000	0.423E-04 ± 0.269E-05
210.000	0.401E-04 ± 0.208E-05
230.000	0.352E-04 ± 0.190E-05
250.000	0.304E-04 ± 0.173E-05
270.000	0.196E-04 ± 0.131E-05
290.000	0.138E-04 ± 0.106E-05
310.000	0.860E-05 ± 0.808E-06
340.000	0.450E-05 ± 0.417E-06
380.000	0.118E-05 ± 0.203E-06
420.000	0.814E-06 ± 0.167E-06
460.000	0.276E-06 ± 0.969E-07
500.000	0.107E-06 ± 0.612E-07
560.000	0.824E-07 ± 0.383E-07
640.000	0.125E-07 ± 0.150E-07

Table A-III. Continued - caption on first page of table.

Energy (MeV)	Yield (n/MeV-msr-ion)
	9°
25.000	0.699E-05 ± 0.529E-06
35.000	0.936E-05 ± 0.603E-06
45.000	0.113E-04 ± 0.638E-06
55.000	0.111E-04 ± 0.605E-06
65.000	0.127E-04 ± 0.658E-06
75.000	0.145E-04 ± 0.722E-06
85.000	0.152E-04 ± 0.752E-06
95.000	0.164E-04 ± 0.800E-06
105.000	0.170E-04 ± 0.826E-06
115.000	0.170E-04 ± 0.826E-06
125.000	0.173E-04 ± 0.838E-06
135.000	0.168E-04 ± 0.823E-06
145.000	0.166E-04 ± 0.814E-06
155.000	0.169E-04 ± 0.828E-06
165.000	0.162E-04 ± 0.803E-06
175.000	0.155E-04 ± 0.778E-06
185.000	0.147E-04 ± 0.749E-06
195.000	0.148E-04 ± 0.754E-06
210.000	0.131E-04 ± 0.586E-06
230.000	0.116E-04 ± 0.531E-06
250.000	0.956E-05 ± 0.457E-06
270.000	0.694E-05 ± 0.361E-06
290.000	0.515E-05 ± 0.293E-06
310.000	0.365E-05 ± 0.232E-06
340.000	0.200E-05 ± 0.124E-06
380.000	0.868E-06 ± 0.741E-07
420.000	0.419E-06 ± 0.493E-07
460.000	0.217E-06 ± 0.347E-07
500.000	0.144E-06 ± 0.282E-07
560.000	0.433E-07 ± 0.108E-07
640.000	0.370E-07 ± 0.101E-07

Table A-III. Continued - caption on first page of table.

Energy (MeV)	Yield (n/MeV-msr-ion)
	12°
25.000	0.697E-05 ± 0.512E-06
35.000	0.941E-05 ± 0.573E-06
45.000	0.982E-05 ± 0.542E-06
55.000	0.954E-05 ± 0.508E-06
65.000	0.106E-04 ± 0.536E-06
75.000	0.115E-04 ± 0.564E-06
85.000	0.117E-04 ± 0.572E-06
95.000	0.125E-04 ± 0.602E-06
105.000	0.113E-04 ± 0.566E-06
115.000	0.110E-04 ± 0.558E-06
125.000	0.109E-04 ± 0.555E-06
135.000	0.107E-04 ± 0.549E-06
145.000	0.106E-04 ± 0.547E-06
155.000	0.967E-05 ± 0.518E-06
165.000	0.913E-05 ± 0.500E-06
175.000	0.897E-05 ± 0.494E-06
185.000	0.856E-05 ± 0.482E-06
195.000	0.793E-05 ± 0.460E-06
210.000	0.690E-05 ± 0.329E-06
230.000	0.579E-05 ± 0.294E-06
250.000	0.456E-05 ± 0.252E-06
270.000	0.354E-05 ± 0.216E-06
290.000	0.297E-05 ± 0.194E-06
310.000	0.199E-05 ± 0.154E-06
340.000	0.120E-05 ± 0.860E-07
380.000	0.645E-06 ± 0.611E-07
420.000	0.390E-06 ± 0.467E-07
460.000	0.230E-06 ± 0.355E-07
500.000	0.109E-06 ± 0.244E-07
560.000	0.537E-07 ± 0.121E-07
640.000	0.211E-07 ± 0.758E-08

Table A-III. Continued - caption on first page of table.

Energy (MeV)	Yield (n/MeV-msr-ion)
	16°
25.000	0.588E-05 ± 0.350E-06
35.000	0.705E-05 ± 0.376E-06
45.000	0.766E-05 ± 0.371E-06
55.000	0.751E-05 ± 0.352E-06
65.000	0.798E-05 ± 0.365E-06
75.000	0.761E-05 ± 0.352E-06
85.000	0.783E-05 ± 0.362E-06
95.000	0.744E-05 ± 0.348E-06
105.000	0.658E-05 ± 0.321E-06
115.000	0.644E-05 ± 0.318E-06
125.000	0.630E-05 ± 0.315E-06
135.000	0.567E-05 ± 0.293E-06
145.000	0.503E-05 ± 0.271E-06
155.000	0.459E-05 ± 0.254E-06
165.000	0.413E-05 ± 0.237E-06
175.000	0.393E-05 ± 0.232E-06
185.000	0.367E-05 ± 0.222E-06
195.000	0.320E-05 ± 0.204E-06
210.000	0.258E-05 ± 0.138E-06
230.000	0.209E-05 ± 0.121E-06
250.000	0.142E-05 ± 0.954E-07
270.000	0.129E-05 ± 0.904E-07
290.000	0.929E-06 ± 0.747E-07
310.000	0.653E-06 ± 0.613E-07
340.000	0.505E-06 ± 0.392E-07
380.000	0.256E-06 ± 0.267E-07
420.000	0.185E-06 ± 0.224E-07
460.000	0.100E-06 ± 0.163E-07
500.000	0.603E-07 ± 0.126E-07
560.000	0.224E-07 ± 0.544E-08
640.000	0.139E-07 ± 0.429E-08

Table A-III. Continued - caption on first page of table.

Energy (MeV)	Yield (n/MeV-msr-ion)
	20°
25.000	0.454E-05 ± 0.313E-06
35.000	0.594E-05 ± 0.360E-06
45.000	0.562E-05 ± 0.325E-06
55.000	0.516E-05 ± 0.294E-06
65.000	0.561E-05 ± 0.311E-06
75.000	0.559E-05 ± 0.309E-06
85.000	0.528E-05 ± 0.299E-06
95.000	0.511E-05 ± 0.291E-06
105.000	0.502E-05 ± 0.289E-06
115.000	0.430E-05 ± 0.260E-06
125.000	0.422E-05 ± 0.259E-06
135.000	0.369E-05 ± 0.236E-06
145.000	0.322E-05 ± 0.215E-06
155.000	0.282E-05 ± 0.197E-06
165.000	0.280E-05 ± 0.196E-06
175.000	0.236E-05 ± 0.177E-06
185.000	0.222E-05 ± 0.171E-06
195.000	0.176E-05 ± 0.148E-06
210.000	0.152E-05 ± 0.104E-06
230.000	0.125E-05 ± 0.925E-07
250.000	0.122E-05 ± 0.912E-07
270.000	0.828E-06 ± 0.723E-07
290.000	0.691E-06 ± 0.651E-07
310.000	0.445E-06 ± 0.507E-07
340.000	0.314E-06 ± 0.308E-07
380.000	0.205E-06 ± 0.241E-07
420.000	0.151E-06 ± 0.204E-07
460.000	0.700E-07 ± 0.137E-07
500.000	0.393E-07 ± 0.102E-07
560.000	0.130E-07 ± 0.413E-08

Table A-III. Continued - caption on first page of table.

Energy (MeV)	Yield (n/MeV-msr-ion)
	24°
25.000	0.316E-05 ± 0.272E-06
35.000	0.381E-05 ± 0.300E-06
45.000	0.430E-05 ± 0.309E-06
55.000	0.432E-05 ± 0.302E-06
65.000	0.414E-05 ± 0.290E-06
75.000	0.402E-05 ± 0.283E-06
85.000	0.385E-05 ± 0.276E-06
95.000	0.362E-05 ± 0.262E-06
105.000	0.320E-05 ± 0.241E-06
115.000	0.300E-05 ± 0.231E-06
125.000	0.268E-05 ± 0.214E-06
135.000	0.263E-05 ± 0.211E-06
145.000	0.196E-05 ± 0.172E-06
155.000	0.215E-05 ± 0.182E-06
165.000	0.177E-05 ± 0.161E-06
175.000	0.158E-05 ± 0.150E-06
185.000	0.174E-05 ± 0.160E-06
195.000	0.133E-05 ± 0.134E-06
210.000	0.122E-05 ± 0.101E-06
230.000	0.982E-06 ± 0.867E-07
250.000	0.805E-06 ± 0.762E-07
270.000	0.622E-06 ± 0.649E-07
290.000	0.557E-06 ± 0.607E-07
310.000	0.455E-06 ± 0.536E-07
340.000	0.317E-06 ± 0.329E-07
380.000	0.162E-06 ± 0.219E-07
420.000	0.792E-07 ± 0.147E-07
460.000	0.674E-07 ± 0.136E-07
500.000	0.206E-07 ± 0.733E-08
560.000	0.153E-07 ± 0.451E-08
640.000	0.669E-08 ± 0.296E-08

Table A-III. Continued - caption on first page of table.

Energy (MeV)	Yield (n/MeV-msr-ion)
	28°
25.000	0.389E-05 ± 0.335E-06
35.000	0.350E-05 ± 0.300E-06
45.000	0.386E-05 ± 0.308E-06
55.000	0.365E-05 ± 0.286E-06
65.000	0.331E-05 ± 0.263E-06
75.000	0.344E-05 ± 0.271E-06
85.000	0.293E-05 ± 0.241E-06
95.000	0.280E-05 ± 0.232E-06
105.000	0.251E-05 ± 0.215E-06
115.000	0.224E-05 ± 0.199E-06
125.000	0.196E-05 ± 0.182E-06
135.000	0.174E-05 ± 0.167E-06
145.000	0.152E-05 ± 0.152E-06
155.000	0.141E-05 ± 0.144E-06
165.000	0.130E-05 ± 0.137E-06
175.000	0.109E-05 ± 0.123E-06
185.000	0.109E-05 ± 0.123E-06
195.000	0.789E-06 ± 0.100E-06
210.000	0.670E-06 ± 0.702E-07
230.000	0.584E-06 ± 0.644E-07
250.000	0.514E-06 ± 0.595E-07
270.000	0.272E-06 ± 0.406E-07
290.000	0.296E-06 ± 0.427E-07
310.000	0.154E-06 ± 0.295E-07
340.000	0.167E-06 ± 0.229E-07
380.000	0.585E-07 ± 0.126E-07
420.000	0.577E-07 ± 0.125E-07
460.000	0.164E-07 ± 0.651E-08
500.000	0.151E-07 ± 0.626E-08
560.000	0.713E-08 ± 0.304E-08

Table A-III. Continued - caption on first page of table.

Energy (MeV)	Yield (n/MeV-msr-ion)
	32°
25.000	0.288E-05 ± 0.252E-06
35.000	0.345E-05 ± 0.272E-06
45.000	0.345E-05 ± 0.255E-06
55.000	0.306E-05 ± 0.226E-06
65.000	0.263E-05 ± 0.201E-06
75.000	0.240E-05 ± 0.188E-06
85.000	0.218E-05 ± 0.178E-06
95.000	0.202E-05 ± 0.168E-06
105.000	0.206E-05 ± 0.172E-06
115.000	0.166E-05 ± 0.151E-06
125.000	0.151E-05 ± 0.142E-06
135.000	0.133E-05 ± 0.132E-06
145.000	0.101E-05 ± 0.111E-06
155.000	0.978E-06 ± 0.108E-06
165.000	0.105E-05 ± 0.113E-06
175.000	0.919E-06 ± 0.106E-06
185.000	0.872E-06 ± 0.103E-06
195.000	0.596E-06 ± 0.822E-07
210.000	0.615E-06 ± 0.628E-07
230.000	0.357E-06 ± 0.458E-07
250.000	0.322E-06 ± 0.433E-07
270.000	0.223E-06 ± 0.355E-07
290.000	0.209E-06 ± 0.342E-07
310.000	0.143E-06 ± 0.279E-07
340.000	0.982E-07 ± 0.165E-07
380.000	0.705E-07 ± 0.138E-07
420.000	0.377E-07 ± 0.992E-08
460.000	0.144E-07 ± 0.609E-08
500.000	0.402E-08 ± 0.317E-08

Table A-III. Continued - caption on first page of table.

Energy (MeV)	Yield (n/MeV-msr-ion)
	36°
25.000	0.178E-05 ± 0.182E-06
35.000	0.263E-05 ± 0.221E-06
45.000	0.265E-05 ± 0.206E-06
55.000	0.217E-05 ± 0.173E-06
65.000	0.169E-05 ± 0.146E-06
75.000	0.178E-05 ± 0.150E-06
85.000	0.178E-05 ± 0.152E-06
95.000	0.143E-05 ± 0.132E-06
105.000	0.134E-05 ± 0.128E-06
115.000	0.125E-05 ± 0.124E-06
125.000	0.102E-05 ± 0.110E-06
135.000	0.977E-06 ± 0.107E-06
145.000	0.731E-06 ± 0.909E-07
155.000	0.711E-06 ± 0.890E-07
165.000	0.709E-06 ± 0.891E-07
175.000	0.502E-06 ± 0.741E-07
185.000	0.569E-06 ± 0.796E-07
195.000	0.445E-06 ± 0.694E-07
210.000	0.386E-06 ± 0.471E-07
230.000	0.304E-06 ± 0.414E-07
250.000	0.186E-06 ± 0.317E-07
270.000	0.161E-06 ± 0.296E-07
290.000	0.141E-06 ± 0.276E-07
310.000	0.113E-06 ± 0.246E-07
340.000	0.863E-07 ± 0.153E-07
380.000	0.415E-07 ± 0.104E-07
420.000	0.173E-07 ± 0.663E-08
460.000	0.446E-08 ± 0.334E-08

Table A-III. Continued - caption on first page of table.

Energy (MeV)	Yield (n/MeV-msr-ion)
	48°
25.000	0.148E-05 ± 0.124E-06
35.000	0.172E-05 ± 0.133E-06
45.000	0.136E-05 ± 0.106E-06
55.000	0.114E-05 ± 0.904E-07
65.000	0.863E-06 ± 0.736E-07
75.000	0.799E-06 ± 0.699E-07
85.000	0.739E-06 ± 0.667E-07
95.000	0.638E-06 ± 0.609E-07
105.000	0.584E-06 ± 0.579E-07
115.000	0.537E-06 ± 0.553E-07
125.000	0.434E-06 ± 0.486E-07
135.000	0.398E-06 ± 0.461E-07
145.000	0.295E-06 ± 0.384E-07
155.000	0.267E-06 ± 0.364E-07
165.000	0.236E-06 ± 0.343E-07
175.000	0.185E-06 ± 0.299E-07
185.000	0.149E-06 ± 0.265E-07
195.000	0.105E-06 ± 0.220E-07
210.000	0.123E-06 ± 0.176E-07
230.000	0.710E-07 ± 0.131E-07
250.000	0.644E-07 ± 0.124E-07
270.000	0.497E-07 ± 0.108E-07
290.000	0.265E-07 ± 0.777E-08
310.000	0.152E-07 ± 0.586E-08
340.000	0.911E-08 ± 0.320E-08
380.000	0.363E-08 ± 0.199E-08

Table A-III. Continued - caption on first page of table.

Energy (MeV)	Yield (n/MeV-msr-ion)
	56°
25.000	0.128E-05 ± 0.994E-07
35.000	0.121E-05 ± 0.922E-07
45.000	0.101E-05 ± 0.760E-07
55.000	0.935E-06 ± 0.692E-07
65.000	0.723E-06 ± 0.581E-07
75.000	0.586E-06 ± 0.511E-07
85.000	0.420E-06 ± 0.422E-07
95.000	0.418E-06 ± 0.423E-07
105.000	0.331E-06 ± 0.373E-07
115.000	0.304E-06 ± 0.358E-07
125.000	0.226E-06 ± 0.306E-07
135.000	0.208E-06 ± 0.292E-07
145.000	0.188E-06 ± 0.274E-07
155.000	0.141E-06 ± 0.237E-07
165.000	0.120E-06 ± 0.219E-07
175.000	0.695E-07 ± 0.165E-07
185.000	0.760E-07 ± 0.173E-07
195.000	0.718E-07 ± 0.168E-07
210.000	0.637E-07 ± 0.114E-07
230.000	0.228E-07 ± 0.671E-08
250.000	0.220E-07 ± 0.661E-08
270.000	0.643E-08 ± 0.351E-08
290.000	0.775E-08 ± 0.388E-08

Table A-III. Continued - caption on first page of table.

Energy (MeV)	Yield (n/MeV-msr-ion)
	72°
25.000	0.760E-06 ± 0.574E-07
35.000	0.566E-06 ± 0.467E-07
45.000	0.520E-06 ± 0.405E-07
55.000	0.369E-06 ± 0.318E-07
65.000	0.277E-06 ± 0.268E-07
75.000	0.233E-06 ± 0.245E-07
85.000	0.182E-06 ± 0.217E-07
95.000	0.139E-06 ± 0.189E-07
105.000	0.142E-06 ± 0.193E-07
115.000	0.129E-06 ± 0.185E-07
125.000	0.551E-07 ± 0.120E-07
135.000	0.438E-07 ± 0.107E-07
145.000	0.385E-07 ± 0.993E-08
155.000	0.506E-07 ± 0.115E-07
165.000	0.379E-07 ± 0.100E-07
175.000	0.163E-07 ± 0.653E-08
185.000	0.211E-07 ± 0.742E-08
195.000	0.582E-08 ± 0.385E-08
210.000	0.740E-08 ± 0.311E-08
230.000	0.348E-08 ± 0.212E-08
250.000	0.170E-08 ± 0.144E-08
270.000	0.841E-09 ± 0.962E-09
290.000	0.339E-08 ± 0.210E-08

Table A-III. Continued - caption on first page of table.

Energy (MeV)	Yield (n/MeV-msr-ion)
	80°
25.000	0.406E-06 ± 0.406E-07
35.000	0.372E-06 ± 0.373E-07
45.000	0.317E-06 ± 0.312E-07
55.000	0.226E-06 ± 0.244E-07
65.000	0.189E-06 ± 0.218E-07
75.000	0.138E-06 ± 0.183E-07
85.000	0.108E-06 ± 0.162E-07
95.000	0.106E-06 ± 0.161E-07
105.000	0.575E-07 ± 0.118E-07
115.000	0.444E-07 ± 0.104E-07
125.000	0.300E-07 ± 0.858E-08
135.000	0.353E-07 ± 0.931E-08
145.000	0.162E-07 ± 0.619E-08
155.000	0.928E-08 ± 0.468E-08
165.000	0.102E-07 ± 0.497E-08
175.000	0.173E-07 ± 0.652E-08
185.000	0.505E-08 ± 0.346E-08
195.000	0.680E-08 ± 0.406E-08
210.000	0.334E-08 ± 0.199E-08
230.000	0.987E-08 ± 0.352E-08
250.000	0.339E-08 ± 0.204E-08
270.000	0.190E-08 ± 0.150E-08

Table A-III. Continued - caption on first page of table.

Ernest Orlando Lawrence Berkeley National Laboratory
One Cyclotron Road | Berkeley, California 94720

Prepared for the U.S. Department of Energy under Contract No. DE-AC03-76SF00098